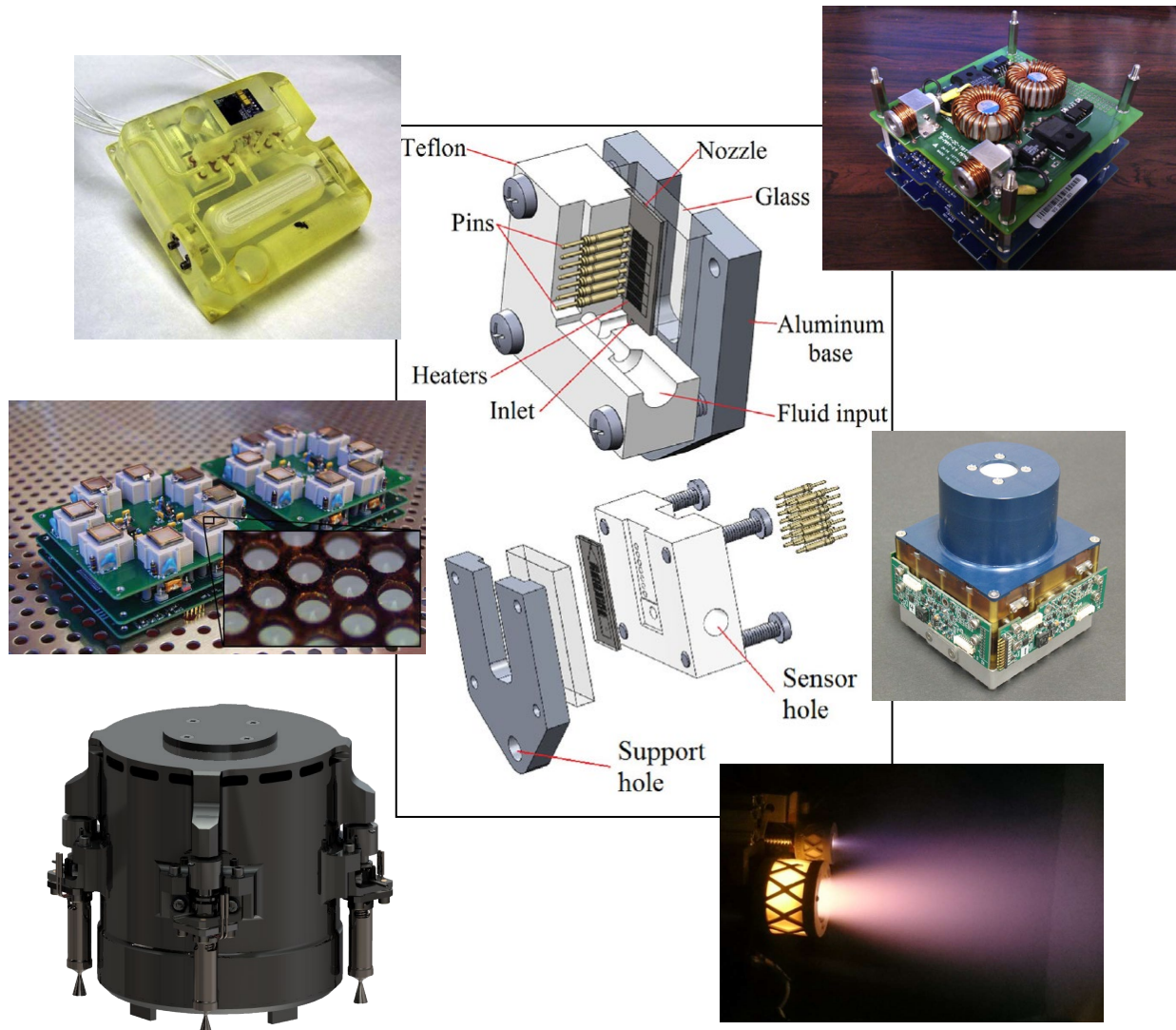


AE4S07 – Course reader

Micro-Propulsion



Dr. A. Cervone

V4.0 - June 2022

Preface

The Micropropulsion course (AE4S07) is offered to TU Delft MSc students, with particular focus on those enrolled in the Space Engineering profile. The first part of the course (to which these lecture notes are explicitly referred) is about the fundamentals of micro-propulsion, in particular:

1. Fundamental theory and state-of-art of micro-propulsion systems for small satellites.
2. Down-scaling and applications of miniaturized propulsion systems and components.

At the end of the first part, after showing in an interim individual test their understanding of the material taught in these lecture notes, the students will be admitted to an individual project (3 ECTS), chosen by the student from a list of options regularly updated by the responsible instructor and aligned with the current micro-propulsion research at TU Delft.

A special acknowledgment goes to all the MSc students who have contributed to updating the micro-propulsion systems database in this report through their Micropropulsion course projects in 2020 and 2021. Particular thanks to Wesley De Vries for his very extensive collection of data on state-of-art electrical micro-propulsion systems.

Specific Learning Objectives (*At the end of this course, the student is able to...*)

- Understand the basics of micro-propulsion systems for small satellites and their fundamental differences to larger scale space propulsion.
- Apply the basic theory to identify the most important requirements for a micro-propulsion system, starting from the relevant top-level mission and satellite requirements.
- Understand and apply down-scaling rules for the miniaturization of propulsion and fluidic systems.
- Know, compare and apply (if required by the specific individual project taken by the student) the main available manufacturing techniques for micro-propulsion systems and components, their range of applicability and their advantages/drawbacks.
- Critically analyze the available state-of-art micro-propulsion options, identify their peculiar characteristics and ranges of applicability, discuss and justify the most suitable one(s) based on given mission and satellite requirements.
- Actively contribute to solve the challenges and achieve the goals of the current micro-propulsion research in the SSE section, by performing the tasks of a specific project, chosen among the ones proposed by the responsible instructor.
- Acquire hands-on skills on one or more of the following (depending on the specific individual project selected by the student): micro-propulsion laboratory and testing activities; design of micro-propulsion systems and components; micro-propulsion verification/optimization by means of analytical or numerical tools; or combinations of the above.

Nomenclature

Abbreviation	Description
ADN	Ammonium DiNitramide
DC	Direct Current
DSSP	Digital Solid State Propulsion
ESA	European Space Agency
FMMR	Free Molecular Micro-Resistojet
HAN	Hydroxyl-Ammonium Nitrate
JPL	Jet Propulsion Laboratory
LEO	Low Earth Orbit
LPM	Low Pressure Micro-resistojet
MEMS	Micro-Electrical Mechanical Systems
MIT	Massachusetts Institute of Technology
NHMF	Non-toxic Homogeneous Miscible Fuel
PPT	Pulsed Plasma Thruster
PTFE	PolyTetraFluoroEthylene (Teflon)
RF	Radio-Frequency
SSTL	Surrey Satellite Technology Ltd
UTIAS	University of Toronto – Institute for Aerospace Studies
1U	1-unit CubeSat
3U	3-units CubeSat
3p	3-units PocketQube
12U	12-units CubeSat

Symbol	Description	SI Units
<i>(Latin)</i>		
a	Speed of sound Regression rate temperature coefficient	m/s m/(s·Pa ⁿ)
A	Frontal area	m ²
A_b	Burning surface solid propellant grain	m ²
A_e	Propellant exhaust area	m ²
A^*	Nozzle throat area	m ²
c_{pG}	Constant pressure specific heat gas	J/(K·kg)
c_{pL}	Constant pressure specific heat liquid	J/(K·kg)
C_d	Drag coefficient	-
d^*	Nozzle throat diameter	m
d_1, d_2	Small spacecraft dimensions	m
D	Hole diameter	m
D_M	Residual dipole	Am ²
e_I	Ionization losses	eV
e_L	Generic losses in an ion thruster	eV
F_T	Thrust	N
I_{sp}	Specific impulse	s
I_x, I_y, I_z	Principal moments of inertia	kg· m ²
L	Distance between grids	m
L_h	Latent heat of vaporization	J/kg
\dot{m}	Mass flow rate	kg/s
M_0	Initial spacecraft mass	kg
M_{dry}	Dry mass of propulsion system	kg

M_P	Propellant mass	kg
M_T	Propellant mass in the tank	kg
M_W	Molecular mass	g/mol
n	Number of holes Solid propellant combustion index	- -
p_a	Ambient pressure	Pa
p_c	Chamber pressure	Pa
p_e	Propellant exhaust pressure	Pa
p_T	Tank pressure	Pa
P	Propulsion system power	W
P_h	Heating power	W
P_{sat}	Average satellite power	W
r	Regression rate	m/s
R	Orbit radius	m
Re^*	Reynolds number at throat	-
t_{life}	Spacecraft lifetime	s
t_b	Burn time	s
T	Orbital period	s
T_{boil}	Boiling temperature	K
T_C	Chamber temperature	K
T_g	Gravity gradient disturbance torque	Nm
T_m	Magnetic field disturbance torque	Nm
T_0	Initial propellant temperature	K
V	Voltage Orbital velocity	V m/s
v_e	Jet velocity	m/s
v_{eq}	Equivalent (or effective) jet velocity	m/s
(Greek)		
ΔR_{man}	Orbital radius correction per maneuver	m
ΔR_{rev}	Orbital radius variation per orbit	m
Δv	Velocity change	m/s
ΔV_{man}	Delta-V per maneuver	m/s
ΔV_{rev}	Orbital velocity variation per orbit	m/s
γ	Specific heat ratio	-
η	Efficiency	-
η_{ion}	Ionization efficiency	-
ν	Kinematic viscosity	m^2/s
θ_{max}	Maximum allowed deviation angle	deg
ρ	Atmospheric density	kg/m^3
ρ_p	Solid propellant grain density	kg/m^3

Important Constants

Definition	Symbol	Value
Electron charge	e	$1.6022 \cdot 10^{-19} \text{ C}$
Earth's gravitational acceleration at sea level	g_0	9.81 m/s^2
Earth's gravity constant	μ	$3.986 \cdot 10^{14} \text{ m}^3/\text{s}^2$
Earth's magnetic moment	M_E	$7.96 \cdot 10^{15} \text{ T} \cdot \text{m}^3$
Avogadro constant	N_A	$6.0221 \cdot 10^{23} \text{ mol}^{-1}$
Universal gas constant	R_A	$8314 \text{ J/(K} \cdot \text{kmol)}$
Earth's radius	R_E	$6.378 \cdot 10^6 \text{ m}$
Permittivity of vacuum	ϵ_0	$8.8542 \cdot 10^{-12} \text{ Farad/m}$

Contents

PREFACE.....	II
NOMENCLATURE	III
CONTENTS	V
1 – INTRODUCTION AND FUNDAMENTALS	1
1.1 Basic space propulsion theory.....	2
1.2 What is “micro”?.....	5
1.3 Down-scaling challenges.....	5
2 – MICRO-PROPULSION STATE-OF-THE-ART.....	9
2.1 Cold Gas systems	9
2.2 Mono-Propellant systems	11
2.3 Bi-Propellant systems	12
2.4 Solid Propellant systems	13
2.5 Micro-Resistojets	14
2.6 Ion thrusters and Radio-Frequency electric thrusters	16
2.7 Hall Effect thrusters	18
2.8 Electrospray thrusters	19
2.9 Pulsed Plasma Thrusters.....	20
2.10 General overview and conclusions.....	22
3 – APPLICATIONS TO SMALL SATELLITES.....	34
3.1 Boundaries of the study: applications and small satellite formats considered.....	34
3.2 Attitude control of an Earth-pointing satellite in LEO	35
3.3 Drag compensation for altitude maintenance in LEO	39
3.4 Station keeping in GEO.....	42
3.5 Interplanetary transfer – Low Lunar Orbit to halo orbit.....	44
3.6 Interplanetary transfer – Mars Transfer Orbit to Low Mars Orbit	46
3.7 Summary and conclusions	48
REFERENCES.....	51

1 – Introduction and Fundamentals

In space engineering, as well as many other areas (microfluidics, medical implants, sensor technology, etc.), the advantages of investing in the **miniaturization** of sub-systems and components are evident. For a spacecraft, saving even a small fraction of mass and volume contributes to make its access to space **easier, cheaper** and **faster**, mitigating some of the problems caused by the significant reductions experienced in recent years on the available budget and launch opportunities for space missions.

One of the most well-known and successful examples of spacecraft miniaturization is represented by the **CubeSat**. When this popular standard was introduced at the end of last century, from the intuition of a group of visionary professors at Caltech and Stanford University, its inventors proposed it as a platform for education and small, low-cost space experiments [1]. Although initially restricted to this very limited field of applications, in recent years the capabilities of CubeSats have rapidly grown. Constellations or swarms of CubeSats have started to be proposed for a wide range of more ambitious applications, ranging from Earth observation to space debris mitigation and high-risk, high-gain scientific missions impossible to be realized with a single, larger spacecraft. The consequence has been a rapidly increasing trend of CubeSat launches, as shown by Figure 1. This trend has become even more evident in recent years, when private companies have started to launch large constellations of CubeSats in Low Earth Orbit for Earth imaging (*Flock* constellation from the company Planet) or for weather/ship tracking (*Lemur* constellation from the company Spire).

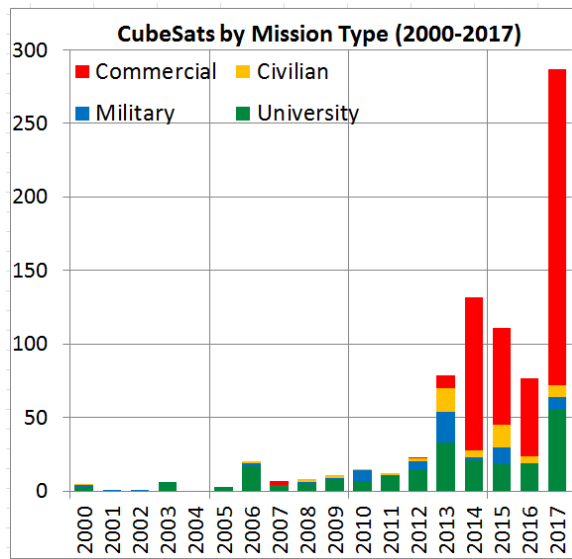


Figure 1: CubeSats launched per year in the period 2000-2017 (data from [2]).

However, a very large portion of the CubeSats currently in orbit does not make use yet of any propulsion system, mainly due to the current lack of a sufficient range of reliable and performing **micro-propulsion** options for this class of satellites. Flying without propulsion intrinsically limits the capabilities of the satellite, with consequences ranging from reduced lifetime in lower altitude orbits to limited formation flying maintainability and no orbit maneuverability. For this reason, research and development activities on micro-propulsion systems are recently attracting more and more attention in universities, research centres and companies. This reader will give an overview on the fundamentals of micro-propulsion theory and the current state-of-art of micro-propulsion research. In the last Chapter, applicability of the current state-of-art micro-propulsion options to some specific missions and applications will be assessed in detail.

1.1 Basic space propulsion theory

It is not the scope of this reader to provide an in-depth overview of the general theory of space propulsion, for which you can find more details in other TU Delft courses such as “Propulsion and Power” (AE2230-II) in the BSc program and “Thermal Rocket Propulsion” (AE4S01) in the Spaceflight MSc track. Here, only some basics will be given, which are considered particularly useful for a better understanding of the material presented in this reader. Consequently, most of the performance equations will be presented without an in-depth explanation of the theory and assumptions behind their derivation.

We usually refer to rocket engines or space thrusters as pure reaction systems, where an amount of propellant is expelled at high speed in a direction opposite to the direction of flight, generating thrust in accordance to Newton’s third law of motion. The most important performance parameters that characterize a space propulsion system are the **thrust**, the **specific impulse** and the **Delta-V**.

The thrust is simply the force produced by the rocket, which can be calculated using the following equation:

$$F_T = \dot{m} \cdot v_e + (p_e - p_a) \cdot A_e = \dot{m} \cdot v_{eq} \quad (1.1)$$

where F_T is the thrust, \dot{m} is the mass flow rate of propellant, v_e is the velocity at which the propellant is expelled relative to the rocket (or *jet velocity*), p_e is the pressure at which the propellant is expelled, p_a is the external ambient pressure, A_e is the propellant exhaust area. Equation (1.1) shows that the thrust is made of two different contributions: a “momentum term” (actual momentum exchange between propellant and spacecraft), and a “pressure term” (difference in pressure between the expelled propellant and the external ambient). In order to write the thrust equation in a more compact way, an *equivalent jet velocity* is usually defined, indicated by v_{eq} in equation (1.1), which accounts for both the momentum and pressure terms in the equation.

The pressure term is a function of the ambient pressure and, thus, the altitude at which the system is flying: it can lead to a significant reduction in thrust (down to 15-20% less thrust) at very low altitudes, but it is usually negligible in vacuum, where basically the equivalent jet velocity is the same as the jet velocity, provided that the exit pressure is as close as possible to zero (or, as it is usually said, the propellant expansion is “adapted” to vacuum conditions). This is the case for all the micro-propulsion systems discussed in this reader, which are supposed to work under vacuum conditions in orbit.

The specific impulse is defined as the ratio of the total impulse generated by the rocket (thrust integrated over the burn time), to the total weight of propellant used to generate it. It is typically measured in seconds, and gives a measure of the propellant consumption efficiency of the system: higher specific impulse means that a higher total impulse is generated with the same propellant mass (or, alternatively, the same total impulse can be obtained by using less propellant). If the equivalent jet velocity is constant over time, the specific impulse I_{sp} can be simply written as:

$$I_{sp} = \frac{v_{eq}}{g_0} \quad (1.2)$$

where g_0 is always the gravitational acceleration on Earth at sea level ($= 9.81 \text{ m/s}^2$), regardless of the place where the rocket or spacecraft is flying.

The Delta-V is the ideal velocity change experienced by the spacecraft in which the propulsion system is installed, when a given mass of propellant has been expelled. It is usually calculated by means of the *rocket equation*, or *Tsiolkovsky equation* (from the name of the scientist who derived it for the first time):

$$\Delta v = v_{eq} \cdot \ln\left(\frac{M_0}{M_0 - M_p}\right) \quad (1.3)$$

The rocket equation gives the velocity change of a spacecraft with initial mass M_0 , when a mass M_p of propellant is expelled by its propulsion system with a given equivalent jet velocity. However, this is only true under a number of assumptions: no external forces acting on the spacecraft (such as gravity or atmospheric drag); equivalent jet velocity constant over time; propellant expelled in a direction exactly opposite to the flight direction. When at least one of these assumptions is not met, the Delta-V calculated by means of the rocket equation is no longer the actual velocity change of the spacecraft; however, it is still a good indicator of the energy transferred by the propulsion system to the spacecraft.

Equations (1.1), (1.2) and (1.3) show that, in order to define in a sufficiently accurate way the performance of a propulsion system, it is important to find equations for three important parameters: the **jet velocity**, the **mass flow rate** and the **propellant exhaust pressure**.

For systems based on thermal expansion of the propellant in a nozzle, simplified equations for these three parameters are provided by the so-called Ideal Rocket Theory. This theory is based on a number of simplifying assumptions for the flow in the nozzle, the most important of which are:

- The fluid flowing in the nozzle is a perfect, calorically ideal gas of constant homogeneous chemical composition;
- Flow is steady, isentropic, mono-dimensional, with purely axial velocity;
- No friction or other external forces act on the gas flowing in the nozzle.

The nozzle is convergent-divergent, with an inlet section in which the flow is considered under stagnation conditions (negligible velocity), a throat section where the flow is sonic, and the exhaust section where the flow is typically highly supersonic.

In spite of the large number of assumptions and simplifications on which it is based, the Ideal Rocket Theory is still surprisingly accurate in evaluating the performance of the nozzle, with results that normally stay within 10-15% from the actual values.

Under the Ideal Rocket Theory assumptions, it is possible to derive the following equation for the jet velocity:

$$v_e = \sqrt{\frac{2\gamma}{\gamma-1} \cdot \frac{R_A}{M_w} \cdot T_C \cdot \left[1 - \left(\frac{p_e}{p_c} \right)^{\frac{\gamma-1}{\gamma}} \right]} \quad (1.4)$$

where p_c and T_c are the pressure and temperature at the nozzle inlet (which is the combustion chamber, in chemical engines), R_A is the universal gas constant ($= 8314 \text{ J/K} \cdot \text{kmol}$), M_w and γ are the molecular mass and specific heat ratio of the gas flowing in the nozzle.

Equation (1.4) shows that higher jet velocity (thus, higher specific impulse) can be achieved by selecting a propellant that allows for higher chamber temperature and lower molecular mass of the gas flowing in the nozzle (which, in chemical engines, is a mix of the products of the chemical reaction in the chamber).

For the mass flow rate, the following equation holds:

$$\dot{m} = \frac{p_c \cdot A^*}{\sqrt{\frac{R_A}{M_w} \cdot T_c}} \cdot \sqrt{\gamma \cdot \left(\frac{1+\gamma}{2} \right)^{\frac{1+\gamma}{1-\gamma}}} \quad (1.5)$$

where A^* is the nozzle throat area.

Finally, the following relationship holds between the area ratio A_e/A^* and the pressure ratio p_c/p_e :

$$\frac{A_e}{A^*} = \frac{\sqrt{\gamma \cdot \left(\frac{1+\gamma}{2}\right)^{\frac{1+\gamma}{1-\gamma}}}}{\sqrt{\frac{2\gamma}{\gamma-1} \cdot \left(\frac{p_e}{p_c}\right)^{\frac{2}{\gamma}} \cdot \left[1 - \left(\frac{p_e}{p_c}\right)^{\frac{\gamma-1}{\gamma}}\right]}} \quad (1.6)$$

For electric propulsion options, where the propellant is accelerated by means of electrostatic or electromagnetic forces, it is more difficult to provide a “universal” set of equations for the thruster performance. A good indication of the parameters that play a major role in influencing the performance can however be obtained looking at the ideal equations for an *ion thruster*, where an electrostatic field between two grids is used to accelerate charged particles and generate the thrust. The charged particles are usually obtained by ionization of the propellant. The thrust is normally not generated by acceleration of the electrons themselves, since they have a very small mass and would not produce enough mass flow rate to generate a useful thrust level.

A simplified equation for the jet velocity of the expelled ions can be written under the assumptions that only single-charged ions are present in the flow and that the kinetic energy acquired by an ion is exactly equal to the energy provided by the electrostatic field by which it is accelerated. The jet velocity can then be calculated as:

$$v_e = \sqrt{\frac{2eN_A V}{M_w}} \quad (1.7)$$

where V is the voltage difference of the electrostatic field between the two grids through which the ions are accelerated, N_A is the Avogadro constant ($= 6.0221 \cdot 10^{23} \text{ mol}^{-1}$) and e is the electrical charge of an electron ($= 1.6022 \cdot 10^{-19} \text{ C}$).

The thrust produced by the ion thruster can be then written as:

$$F_T = \frac{2\pi\varepsilon_0}{9} \cdot V^2 \cdot n \left(\frac{D}{L}\right)^2 \quad (1.8)$$

where n is the number of holes in the grids, L is the distance between the grids, D is the diameter of each hole in the grid, and ε_0 is the permittivity of vacuum ($= 8.8542 \cdot 10^{-12} \text{ Farad/m}$).

The specific impulse of an ion thruster can be calculated as:

$$I_{sp} = \eta_{ion} \cdot \frac{v_e}{g_0} = \frac{\eta_{ion}}{g_0} \cdot \sqrt{\frac{2eN_A V}{M_w}} \quad (1.9)$$

where η_{ion} is the ionization efficiency, which accounts for the fact that not all propellant atoms are ionized and contribute in an effective way to generate thrust, and has a typical value in the order of 0.7-0.9 in most ion thrusters.

Finally, the thruster efficiency (ratio of kinetic power in the exhaust jet to input power provided to the thruster by the power plant) can be written as:

$$\eta = \frac{\frac{1}{2} \frac{M_w}{N_A} v_e^2}{\frac{1}{2} \frac{M_w}{N_A} v_e^2 + e_I + e_L} \quad (1.10)$$

Where e_I is the ionization potential (energy needed for ionizing one atom of propellant) and e_L is a term which accounts for all other energy losses in the system.

Looking at equation (1.10) it is clear that, differently to propulsion systems where the propellant is accelerated in a nozzle, the ideal propellant for an ion thruster is a fluid with high molecular mass and low ionization potential. In this way, less energy is needed to ionize a heavier atom and, thus, to produce a higher mass flow rate of ions.

1.2 What is “micro”?

The definition of “micro-propulsion” is not as trivial as it might seem. The word “micro”, when used in combination with “propulsion”, may have at least two different meanings. It may mean low thrust, which is typically referring to a thrust level from the μN scale to several mN , or small size, in the range of a few cm (or even, for very miniaturized cases, mm) for the whole propulsion system.

In this reader, both definitions will be used, sometimes separately or in other cases combined, mainly depending on the **application** for which the micro-propulsion system is considered and its specific requirements (see Chapters 2 and 3 for more details on the different types of available micro-propulsion systems and their range of applications).

1.3 Down-scaling challenges

In systems based on thermal expansion of the propellant in a nozzle, the main down-scaling challenge when trying to reduce the thrust level to the mN range or lower is represented by the efficiency of the nozzle itself. An example is shown in Figure 2, taken from Bayt [3], which compares the discharge coefficient obtained from numerical simulations and from experiments for two different conical nozzles: the left hand side plot is referred to a nozzle with area ratio of 7 and throat size of $34 \mu\text{N}$, the right hand side plot is for a nozzle with area ratio of 15.3 and throat size of $18 \mu\text{N}$. The “discharge coefficient” is defined here as the ratio of the actual measured (or calculated) mass flow rate to the nominal one obtained by means of the Ideal Rocket Theory; thus, a low discharge coefficient indicates the presence of significant losses in the nozzle flow.

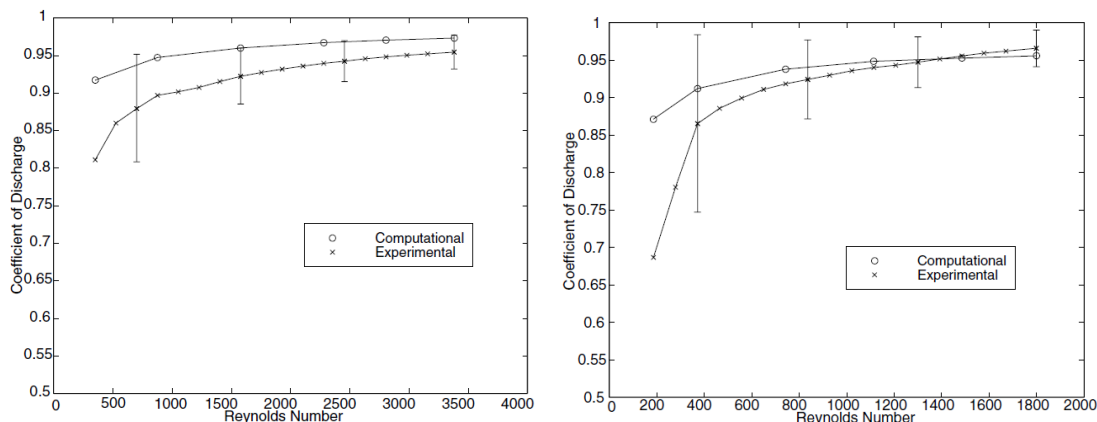


Figure 2: Comparison between the discharge coefficient obtained from numerical simulations and from experiments, for two different conical nozzles using Nitrogen at an external ambient pressure of 4 kPa (from [3]).

In both the plots, the discharge coefficient is shown as a function of the **Reynolds number** Re^* at the nozzle throat, which is defined as:

$$Re^* = \frac{a \cdot d^*}{\nu} \quad (1.11)$$

where a is the speed of sound and ν the kinematic viscosity of the gas flowing in the nozzle (evaluated at throat conditions in terms of pressure and temperature), and d^* is the throat diameter.

Besides the significant uncertainty in the experimental results, reported by the author to be caused by a combination of uncertainty of measurements and inaccuracy of micro-nozzle manufacturing, the plots in Figure 2 clearly show a dramatic decrease in nozzle performance starting at a throat Reynolds number in the range 500-1000. The reason behind this performance drop is not fully understood yet, but is believed to be related to the thick boundary layer at the nozzle throat caused by the laminar flow, which in turns makes the effective throat area smaller and the mass flow rate lower than the ideal one, see equation (1.5). This also makes the expansion in the nozzle divergent less effective due to the separation effects, with a worst case in which no expansion at all occurs when the flow separation becomes large enough. It is therefore expected that conventional nozzle shapes would not work properly at a throat Reynolds number lower than 1000, for which different types of nozzle shapes would need to be considered.

Recent research conducted at TU Delft [18] has shown that for this range of very low throat Reynolds number, **aerospike** micro-nozzles (i.e., nozzles with the flow expanding around a central solid body, instead of being bounded by external walls) can allow for a performance improvement up to 33% when compared to conventional convergent-divergent ones.

It is now possible to assess how these considerations reflect in the design and scaling of micro-propulsion systems. Recalling that, in micro-propulsion systems, the pressure term in the thrust equation can be neglected, equation (1.1) can be combined with equations (1.4) and (1.5) in the following way:

$$F_T = \dot{m} \cdot v_e \propto p_C A^* \propto p_C (d^*)^2 \quad (1.12)$$

In a similar way, for the throat Reynolds number as defined in equation (1.11), it is possible to show that:

$$Re^* = \frac{a \cdot d^*}{\nu} \propto p_C \cdot d^* \quad (1.13)$$

Equation (1.13) can be derived looking at the relationships for an ideal gas, according to which the speed of sound is proportional to the square root of pressure divided by density, and the kinematic viscosity is inversely proportional to the square root of pressure multiplied by density.

Starting from equations (1.12) and (1.13), assume now that the objective is down-scaling a propulsion system with a thrust reduction by a factor 100 (which means, as an example, lowering it from 0.1 N to 1 mN). A first option would be to keep the chamber pressure constant; according to equation (1.12), this means reducing the throat diameter by a factor 10 which in turn, according to equation (1.13), means that the Reynolds number will also be reduced by a factor 10 with a concrete risk of significantly higher losses in the nozzle (see again Figure 2). Another option would be to reduce the throat diameter by a factor 100 and increase the chamber pressure by the same factor; this would keep the Reynolds number constant, at the cost of an extremely high chamber pressure with all consequent problems in terms of structural strength and system safety.

Another set of important down-scaling issues come from the variations of **heat transfer** mechanisms with size. Heat transfer by conduction becomes much more effective in micro-propulsion systems because, for the same material and the same thermal conductivity, smaller size leads to smaller temperature gradients and, thus, a significantly more uniform temperature in the whole thruster. This may represent an issue especially in thrusters where high temperatures are expected, such as chemical propulsion systems, where a large amount of heat power needs to be released by a smaller volume and, thus, the thermal stresses in the material are amplified. Convective heat transfer between propellant and nozzle also increases, meaning that higher thermal losses can be expected in the nozzle flow. Other design challenges are generated by the significantly different thermal expansion coefficients of different materials used in the thruster, which may lead to increased risk of leaks and

additional thermal stresses. Finally, in propulsion systems where a **chemical reaction** takes place in the combustion chamber, the effectiveness of the chemical reaction strongly depends on the residence time of the propellants in the chamber and on the so-called characteristic length, a design parameter defined as the ratio of the chamber volume to the nozzle throat area. For a given combination of propellants, there is always a (fixed) optimum range of characteristic length values in order to achieve efficient combustion. Considering that the ratio of combustion chamber area to throat area is not expected to change significantly when going from macro- to micro-scale, this means that the combustion chamber length should be kept constant for any size of the system, which is obviously not practical when all other dimensions are reduced by several orders of magnitude.

Example

For the Space Shuttle Main Engine, using general orders of magnitude, we can assume a thrust level in the order of 10^6 N, a throat diameter in the order of 10^{-1} m, a chamber pressure in the order of 10^7 Pa = **100 bar**, a throat Reynolds number in the order of 10^8 .

Starting from these values, what would be the values of throat diameter and throat Reynolds number required to scale down the engine and achieve a thrust level in the **1 N, 1 mN and 1 μ N** range?

We make the following assumptions:

-) To avoid too large structural stresses, the chamber pressure can not be higher than 10^7 Pa (but it can be lower).
-) The chamber temperature, specific heat ratio and expansion ratio remain constant when the engine is scaled down.
-) All down-scaling challenges associated to heat transfer mechanisms, chamber temperature and chemical reaction efficiency will be neglected. This is a strong assumption which will definitely not be met in reality, but is useful to assess what are the down-scaling challenges from a purely fluid dynamic point of view.

To match the given design values for the Space Shuttle Main Engine, equations (12) and (13) can be written as follows:

$$F_T = 10 p_C (d^*)^2 \quad Re^* = 100 p_C \cdot d^*$$

Using these equations, it is possible to plot the relationship between throat diameter, throat Reynolds number, chamber pressure and thrust, as shown in Figure 3.

Keeping the Reynolds number higher than 1000 implies that the thrust level cannot be made lower than 0.1 mN with the given constraints (with however a nozzle throat diameter in the order of 1 μ m), but this minimum thrust value tends to increase up to around 10 mN when the chamber pressure is reduced down to 2 bar (with more reasonable throat diameter values in the range 10-100 μ m).

In practice, given the other constraints associated to temperatures, combustion efficiency and nozzle heat transfer, it is practically very difficult, if not impossible in some cases, to design chemical propulsion systems, especially bi-propellant ones, for a thrust level lower than 0.5-1 N.

For electric micro-propulsion systems, as well as any other micro-propulsion systems that require a non-negligible amount of power for their operation, the most significant down-scaling challenge is represented by the **power** itself as well as, in most of the cases, the **power-to-thrust** ratio.

Consider, just as an example, the electrostatic ion thruster and its governing equations as presented in section 1.1. It is clear from equation (1.9) that the grid voltage difference V shall be kept as constant as possible in order to allow for effective acceleration of the ions and for

preserving a sufficiently high specific impulse. These systems are characterized, already in their non-miniaturized version, by low thrust levels in the mN range; thus, to keep the thrust level in this same range with constant V it is necessary, according to equation (1.8), to keep the same geometry in terms of grid aspect ratio D/L and number of grid holes n . This, in turn, implies that the input power required by the thruster stays of the same order of magnitude, irrespectively on the fact that the thruster and/or the target spacecraft size have been scaled down. As a consequence, it is extremely challenging (as it will be better shown in the next chapters) to design miniaturized versions of electric propulsion systems with a thrust level in the mN range without requiring an unreasonably high amount of input power. Most of the electric propulsion options currently available for CubeSats are therefore targeted for a thrust level in the μN range.

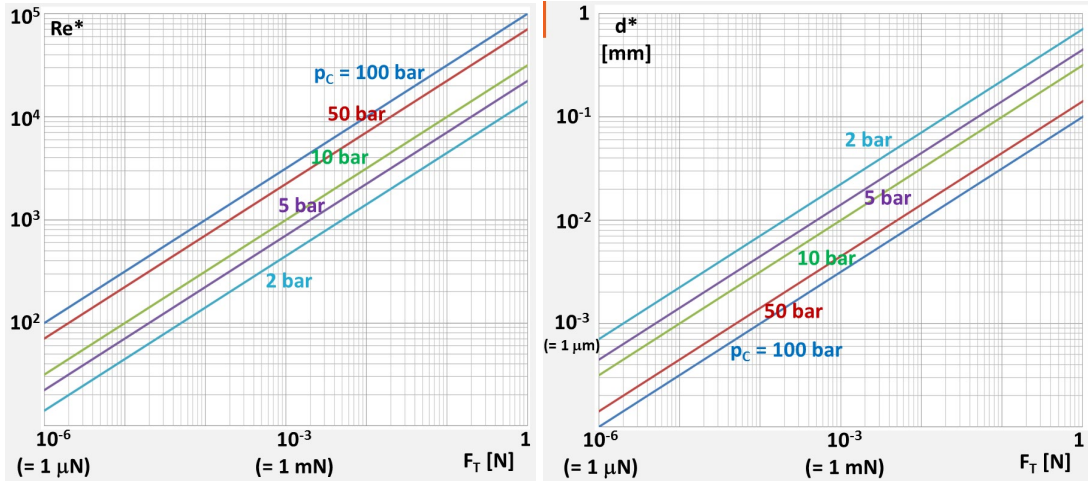


Figure 3: Relationships between nozzle throat diameter, throat Reynolds number, chamber pressure and thrust level for the Space Shuttle Main Engine example case.

2 – Micro-Propulsion State-of-the-Art

In this Chapter, a comprehensive overview will be provided on the current state-of-the-art of micro-propulsion systems (using the word “micro” with its wider meaning, as previously discussed in Section 1.2: either low thrust, or small size, or both).

A large number of recent publications presenting similar overviews are available in literature. The information presented in this Chapter is based, in particular, on the work of Levchenko et al. [4]; [17], Tummala and Dutta [5], Krejci and Lozano [6], Silva et al. [7], Lemmer [8], Parker [9], Leomanni et al. [10]. The data collection has been further updated based on the data gathered by some MSc students for their Micropropulsion course projects in 2020 and 2021. However, given the highly dynamic nature of this research field, new publications presenting updated developments and overviews can be expected in the future; in the same way, it can be expected that some of the specific micro-propulsion systems presented in the following are improved and updated to better performing versions. Finally, in some cases, ambiguous and/or incomplete information on a given micro-propulsion system can be found in literature, and it is not always possible to solve these ambiguities in an easy and definitive way. Nevertheless, the general discussion and conclusions drawn in this Chapter can still be considered fully valid, irrespectively on the missing/ambiguous information and of any possible new developments in the field.

2.1 Cold Gas systems

In cold gas systems, the propellant is stored at high pressure (usually in its liquid phase to allow for higher density and therefore reduced volume, but in principle it can also be stored in the gaseous phase) and accelerated in a nozzle without any additional heating or energy input. If the propellant is stored as a liquid, it is vaporized before reaching the nozzle. Given the simple design and extreme simplicity of the concept, the system mass is usually small and a limited number of components are required. Figure 4 shows a schematic representation of the working principle of a typical cold gas micro-thruster, and its most important components.

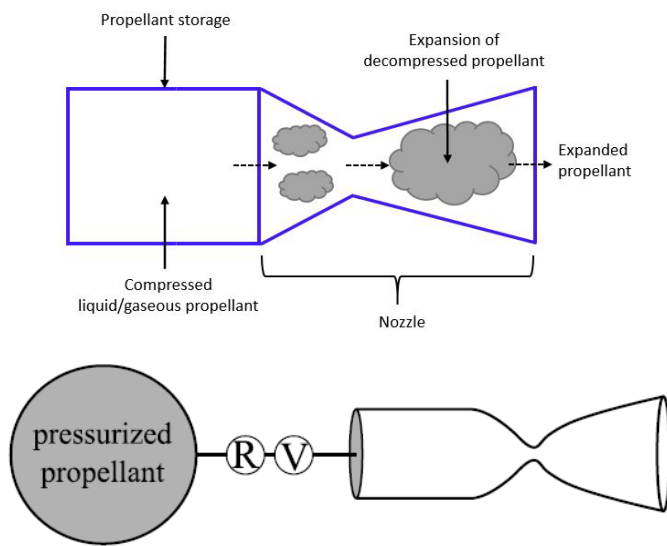


Figure 4: Working principle of a cold gas micro-thruster (top, from [5]) and schematic of its main components (bottom, from [6]).

Although Figure 4 shows a **valve** (V) and **pressure regulator** (R), in micro-thrusters typically the pressure regulator is not present due to mass and volume limitations (in particular when the propellant is stored in the gaseous phase), and the only required power is to activate the valve and keep it open when needed. In absence of the pressure regulator, the gaseous propellant storage pressure in the tank continuously decreases while propellant is

extracted from it (*blow-down* operation). If the extraction of propellant is not too fast, it can be assumed that the blow-down process is isothermal and, therefore, the pressure p_T and mass M_T of propellant in the tank change according to the following relationship:

$$\frac{p_T}{M_T} = \text{constant} \quad (2.1)$$

Since the working principle of cold gas systems is based on accelerating the propellant in a nozzle, the Ideal Rocket Theory equations (1.4), (1.5) and (1.6) apply. Due to the low temperature of the propellant at the nozzle inlet, it is evident from equation (1.4) that in cold gas systems the jet velocity (and, consequently, the specific impulse) is limited. Furthermore, given the continuous reduction of tank pressure in non-regulated systems, and remembering from equation (1.12) that the thrust is proportional to the propellant inlet pressure, it can be inferred that the thrust level provided by these systems is not constant and continuously decreasing with time during operation in orbit.

Typical propellants for cold gas micro-thrusters are **Isobutane, refrigerants** (such as R236fa or R134a), **Sulfur Dioxide, Sulfur Hexafluoride**, but also more common gases such as **Nitrogen, Argon, Xenon**.

Given their simplicity, cold gas micro-thrusters are the ones which have been most widely developed and even, in some cases, successfully operated in space. Flight demonstrated systems include:

- The Nano Propulsion System (**NANOPS**) from the University of Toronto Institute for Aerospace Studies (UTIAS), successfully demonstrated on CanX-2, a 3U CubeSat launched in April 2008. This system was designed specifically for formation flying applications, with a specific impulse of 45 s and a thrust of 50 mN. An updated version, the Canadian Nanosatellite Advanced Propulsion System (**CNAPS**) was launched on a 8U CubeSat, CanX-5, where it was used to perform drift recovery and station keeping. Both these systems used Sulfur Hexafluoride as propellant.
- The five-nozzles cold gas system developed by Aerospace Corporation for the MEMS PICOSAT Inspector (**MEPSI**) launched in 2006. This system, shown in Figure 5, was manufactured using 3D printing technology, so that the propellant tank, pipes and nozzles are all manufactured out of one piece, limiting the leakage risks. The propellant was Xenon. Only one of the five thrusters could be successfully demonstrated in space after satellite deployment.

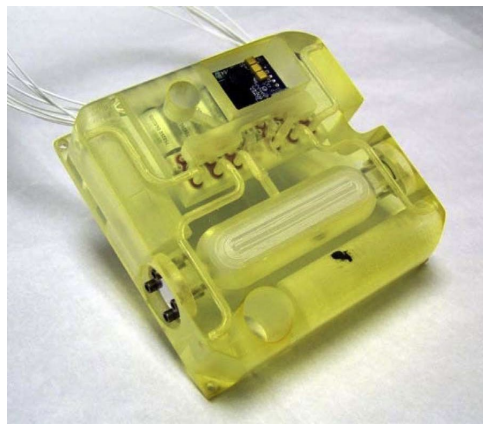


Figure 5: The MEPSI cold gas micro-propulsion system from Aerospace Co. (from [8]).

- The eight-nozzles system developed by Microspace Rapid Ltd (Singapore) for the 3U CubeSat **POPSAT-HIP1**, launched in 2014. The system was intended for formation flight and station keeping purposes, operating with Argon, and successfully performed several maneuvers (angular velocity change, detumbling, attitude change), delivering a total Delta-V of 2.25 m/s.

- The **T3μPS** system developed by TNO, TU Delft and the University of Twente (Netherlands), based on nitrogen propellant stored in solid grains, and partially demonstrated in the Delfi-n3Xt 3U CubeSat in 2013.
- The four-nozzles cold gas system developed by NanoSpace (Sweden) and successfully launched and operated on the microsatellite **PRISMA**. Each nozzle delivered a minimum thrust of 0.1 mN, with specific impulse up to 75 s. The same system can be operated with several different propellants, ranging from liquid water to Xenon, Helium and Nitrogen.

2.2 Mono-Propellant systems

In mono-propellant systems (see Figure 6), the propellant is typically stored in its liquid phase and pressurized by a pressurant gas which is usually stored separately, with a pressure regulator (R) between the two tanks in order to ensure for constant nozzle inlet pressure and, therefore, constant thrust. By opening the thrust valve (V), the propellant is then flown into the decomposition chamber, where it chemically decomposes into simpler molecules generating heat and, therefore, entering the nozzle inlet at high temperature. Decomposition is usually facilitated by a **catalyst**, but also requires in most cases **pre-heating** of the propellant which, in turn, requires a non-negligible amount of satellite power.

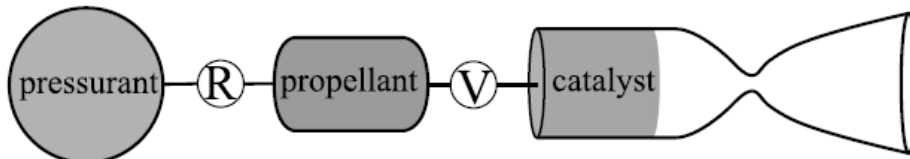


Figure 6: Schematic of a mono-propellant system with its main components (from [6]).

Also in this case, since thrust is generated by accelerating the propellant in a nozzle, the Ideal Rocket Theory equations (1.4), (1.5) and (1.6) apply. The specific impulse is normally significantly higher than cold gas systems, given the higher nozzle inlet temperature of the decomposition gases.

In the case of mono-propellant micro-propulsion systems, “green” propellants are typically used (non-toxic, non-hazardous, easily storables and safe to handle). High-density liquids are usually preferred in order to reduce the required tank volume. Typical propellants are Hydroxyl-Ammonium Nitrate (**HAN**) and its recently developed, high-performance derivative **AF-M315E**; Ammonium DiNitramide (**ADN**) and its derivative **LMP-103S**. A less typically used green alternative is **Hydrogen Peroxide**.

Although some limited flight demonstrations of micro-monopropellant systems have been performed in orbit, the general development status of these systems is less advanced than micro-cold gas systems. However, several systems have been fully developed and are available on the market:

- The CubeSat Modular Propulsion System (**MPS**) developed in several variants by Aerojet Rocketdyne, based on a modular system adapted from a hydrazine version to HAN-based propellants. The MPS-130 (Figure 7, left) is based on four 1 N thrusters with a specific impulse of 240 s.
- The **BGT-X5** system developed by Busek Co. (Figure 7, right), also working with a HAN-based propellant. It is a 0.5 N thruster which requires 15 W of power for catalyst pre-heating. Another version developed by Busek Co. is the **BGT-X1**, which delivers a thrust of 0.1 N.
- Several ADN-based systems have been developed by VACCO. They include the **MiPS** CubeSat system consisting of four 0.1 N thrusters, which can be optionally complemented by lower-thrust cold gas nozzles allowing for thrust misalignment correction.
- Currently, the only available European full mono-propellant micro-propulsion system is the **EPSS C1K**, a system based on ADN propellant which delivers a thrust of 0.1 N, developed by the Lithuanian company NanoAvionics.

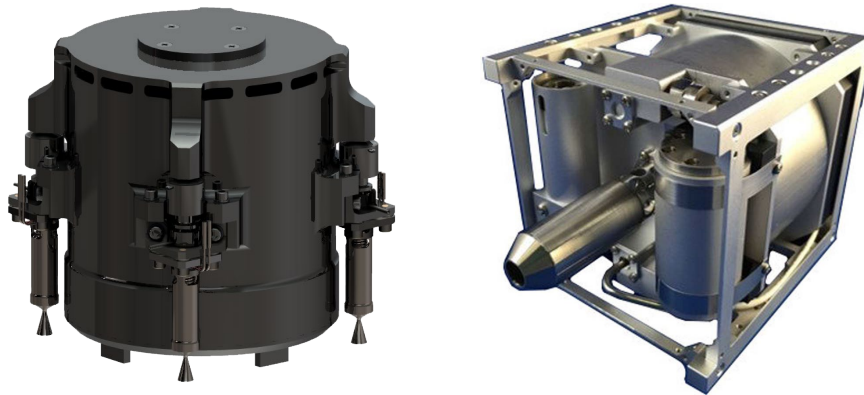


Figure 7: The Aerojet Rocketdyne MPS-130 (left) and the Busek Co. BGT-5X (right, from [8]) mono-propellant systems.

2.3 Bi-Propellant systems

The working principle of bi-propellant systems (Figure 8) is very similar to mono-propellant ones. However, instead of one single propellant there are two of them (an oxidizer and a fuel), also in this case stored in their liquid phase and pressurized by a pressurant gas usually stored separately, with a pressure regulator (R) between the two tanks in order to ensure for constant nozzle inlet pressure and, therefore, constant thrust. Two thrust valves (V) are present in this case, through which the propellants flow into the combustion chamber, where a chemical reaction between fuel and oxidizer generates heat and allows them to enter the nozzle inlet at high temperature. Not many bi-propellant systems are currently available at the micro-scale and they are usually characterized by a relatively high trust level compared to other micro-propulsion systems, mainly due to down-scaling issues related to the residence time of propellants in the combustion chamber, as already described in Chapter 1. It should be noted that the combustion temperature is normally significantly higher than mono-propellant systems, which allows for higher specific impulse but also causes more significant thermal issues.

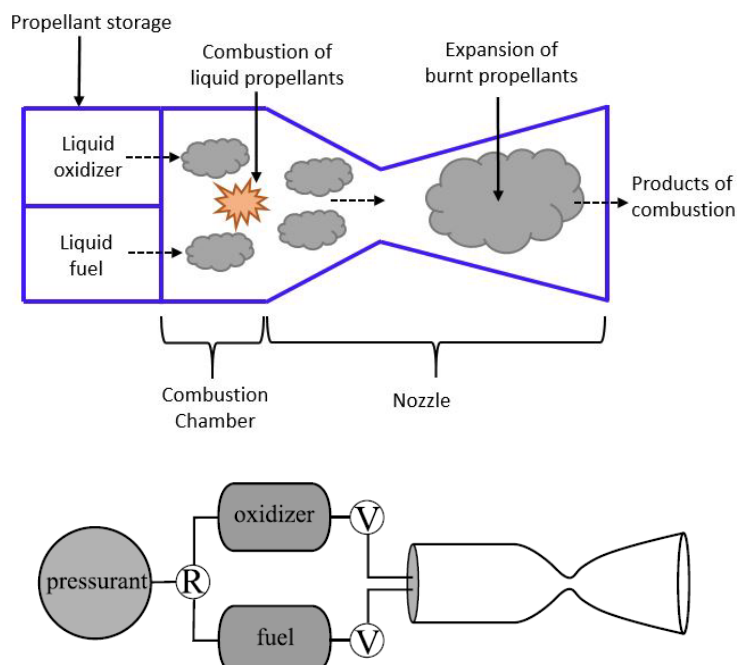


Figure 8: Working principle of a bi-propellant system (top, from [5]) and schematic of its main components (bottom, from [6]).

Once again, since thrust is generated by accelerating the propellant in a nozzle, Ideal Rocket Theory equations (1.4), (1.5) and (1.6) can be used to characterize the thruster performance. Due to the mentioned down-scaling limitations which don't allow for particularly low thrust levels, the number of currently available bi-propellant micro-thruster options is limited. They include:

- The **PM400** and **PM200** produced initially by Hyperion BV and currently by Dawn Aerospace (Netherlands), working with Nitrous Oxide and Propene as propellants and characterized by a specific impulse of 285 s, with thrust levels ranging from 0.5 to 1 N. However, thermal issues due to the high temperatures involved in the combustion process limit the operation of these systems to a few seconds of thrusting time, with significant cooling periods required between an activation and the following one.
- A quite peculiar system is the **HYDROS** micro-thruster (Figure 9), produced by the company Tethers Unlimited. In this system, the propellant is stored as liquid water and electrolysis is used to convert water into hydrogen and oxygen which are the actual fuel and oxidizer flown in the combustion chamber. The thrust level can vary within a relatively wide range, with a nominal value of 1.2 N and specific impulse of 310 s. The dry mass of the system is however affected by the need for a water electrolyzer, which also requires power to be operated (in the range of 5-10 W depending on the required thrust level).

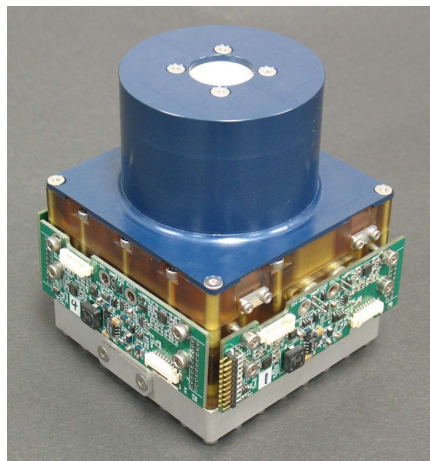


Figure 9: The HYDROS micro-thruster produced by Tethers Unlimited (from [8]).

2.4 Solid Propellant systems

Solid propellant systems (Figure 10) are basically the same as bi-propellant ones, with the only difference that propellants are stored in solid phase in the same grain, and require energy from an igniter to start their combustion. Although extremely simple in terms of number of components and operation, they suffer from the fact that combustion of a single grain, once initiated, can not be stopped and will continue until the propellants are completely consumed. This category of propulsion systems have not been extensively developed yet for small satellites due to the typical limitations on pyrotechnic devices present in the requirements for this class of satellites; however, some systems characterized by significantly high thrust levels (in the range 10-100 N) have been proposed for specific applications, such as de-orbiting at the satellite end of life.

Together with Ideal Rocket Theory equations (1.4), (1.5) and (1.6), still valid as in all systems where propellant is expanded in a convergent-divergent nozzle, the **regression rate** r of the solid propellant grain has to be taken into account. In the simplest possible approximation, the regression rate can be estimated as a function of the combustion chamber pressure through the following equation:

$$r = a \cdot p_C^n \quad (2.2)$$

where a is the temperature coefficient and n is the combustion index (normally lower than 1), both characteristic of the specific solid propellant grain. The mass flow rate can then be calculated as:

$$\dot{m} = r \cdot \rho_p \cdot A_b \quad (2.3)$$

where ρ_p is the propellant grain density and A_b is its instantaneous burning surface. From equations (2.2) and (2.3), it is clear that the chamber pressure evolution over time, and therefore the thrust evolution over time, are a direct consequence of how the grain burning surface changes over time. By selecting a grain geometry with increasing, decreasing or constant burning surface, it is possible to also obtain increasing, decreasing or constant chamber pressure and thrust.

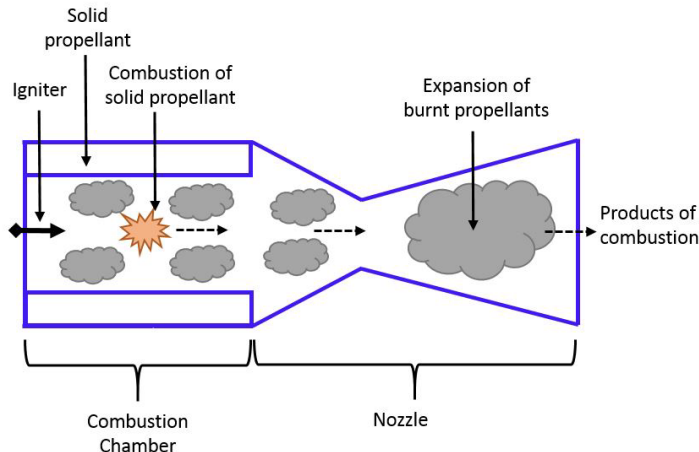


Figure 10: Working principle of a solid propellant micro-thruster (from [5]).

2.5 Micro-Resistojets

Resistojets can be seen as an intermediate concept between electrical and chemical propulsion since, as schematically shown in Figure 11, the propellant is heated electrically (typically by means of a resistance) and accelerated in a convergent-divergent nozzle. In principle, any propellant can be used, stored in any phase (liquid, solid or gaseous); in practice, however, liquid propellants are the most widely used. An alternative to liquid propellants are the so-called *warm gas* thrusters, which are basically cold gas systems allowing for additional (usually limited) heating of the gaseous propellant before being accelerated in the nozzle.

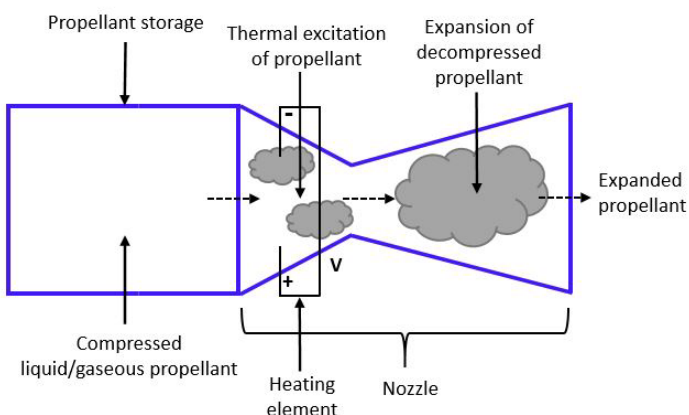


Figure 11: Working principle of a micro-resistojet thruster (from [5]).

In terms of components and operational characteristics, resistojets are very similar to cold gas thrusters: the propellant is stored in a tank, pressurized (when in the liquid phase) by a pressurant gas and injected in the heating chamber by opening a thrust valve. A pressure

regulator is usually not included, meaning that the operation is typically blow-down and the pressure (and thrust) provided by the system are decreasing over its lifetime. The specific impulse, although higher than cold gas systems due to the higher temperature of the propellant and the nozzle inlet, is still limited due to the limitations in the available heating power. Since the propellant is accelerated in a nozzle, equation (1.5) for the mass flow rate is still valid; however, for the most common case of a liquid propellant that needs to be vaporized before being accelerated in the nozzle, it has to be combined with the following relationship that characterizes the vaporization and heating of the propellant:

$$P_h = \dot{m} \cdot [c_{pL} \cdot (T_{boil} - T_0) + L_h + c_{pG} \cdot (T_C - T_{boil})] \quad (2.4)$$

where P_h is the available heating power, T_0 is the initial propellant temperature, T_{boil} is the propellant boiling temperature (which in turn is a function of the heating chamber pressure), c_{pL} and c_{pG} are the constant pressure specific heat of respectively the liquid and gaseous propellant phase (both usually functions of the temperature), L_h is the latent heat of vaporization of the propellant. Combining equations (1.5) and (2.4), it is possible to write the following relationship:

$$P_h = \frac{p_C \cdot A^*}{\sqrt{\frac{R_A}{M_W} \cdot T_C}} \cdot \sqrt{\gamma \cdot \left(\frac{1+\gamma}{2}\right)^{\frac{1+\gamma}{1-\gamma}}} \cdot [c_{pL} \cdot (T_{boil} - T_0) + L_h + c_{pG} \cdot (T_C - T_{boil})] \quad (2.5)$$

Equation (2.5) shows a direct relationship not only between heating power and chamber temperature (as expected), but also between heating power and propellant pressure. This means, in other words, that given a desired temperature at which the propellant has to be heated, the required heating power to achieve that temperature will be a function of the propellant pressure and, therefore, in a system without pressure regulator it will vary over the lifetime of the system. This complicates the design of the control electronics and, at the same time, poses additional limitations on the achievable thrust and specific impulse levels.

TU Delft is currently working at a micro-resistojet system for small satellites using **liquid water** as propellant (Figure 12). The target thrust is in the order of 1 mN and the target specific impulse in the order of 100 s. The choice of water is not only driven by the fact that it is a safe, easy to handle, cheap propellant, but also by a thorough analysis which has shown that, among all propellants that can be stored as a liquid at ambient temperature and relatively low pressure (no more than 10 bar), water is the fluid which allows for the best combination of specific impulse and tank volume for a given Delta-V requirement, thanks to its relatively low molecular mass and high density, in spite of the high value of its heat of vaporization (Guerrieri et al., [13]).

An alternative micro-resistojet concept, sometimes referred as Free Molecular Micro Resistojet (FMMR) or, in the version currently under development at TU Delft, Low Pressure Micro-resistojet (LPM, Guerrieri et al. [14]), operates at a significantly low propellant storage pressure, in the order of a few hundred Pa, in order to work in the free molecular flow regime under non-continuum conditions. In this way, it is not necessary anymore to accelerate the propellant molecules in a nozzle and simple, constant geometry, expansion slots are sufficient; furthermore, the slot walls are heated and therefore the expansion slots also operate as heaters, through interaction with the propellant molecules bouncing on the walls.

Other micro-resistojet options currently under development include:

- The CubeSat High Impulse Propulsion System (**CHIPS**) developed by CU Aerospace and VACCO, for attitude control and primary propulsion of small satellites. The system uses the R134a refrigerant as propellant, with a specific impulse of 76 s and a thrust of 31 mN at 25 W input power.
- The (unnamed) micro-resistojet thruster developed by Busek Co. and using Ammonia as propellant, with a specific impulse of 150 s and a thrust of 10 mN at 9 W input power.

- The **AQUARIUS** water resistojet developed by the University of Tokyo (Japan), demonstrated in the AQT-D spacecraft launched from the International Space Station in 2019, characterized by vaporization of the propellant happening in a separate smaller tank (and not in the thruster itself), with a specific impulse of 70 s and a thrust level of up to 4 mN at approximately 18 W input power.

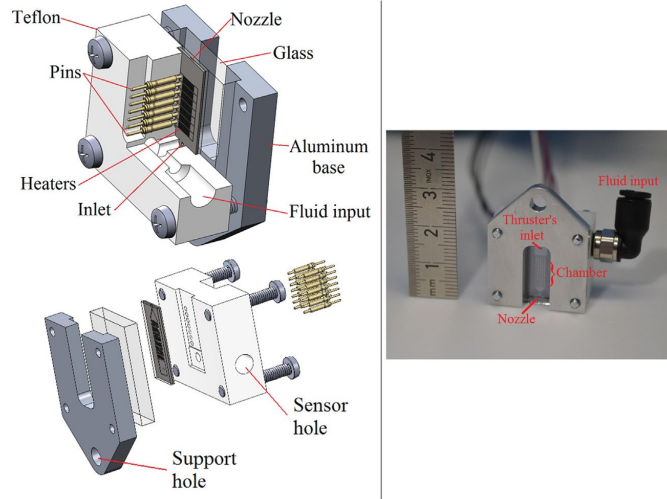


Figure 12: The water micro-resistojet thruster developed by TU Delft (from [12]).

2.6 Ion thrusters and Radio-Frequency electric thrusters

A short explanation of the working principle of ion thrusters has already been given in Chapter 1, where equations (1.7), (1.8), (1.9) and (1.10) have been presented to characterize the performance of this type of propulsion systems. A simplified schematic of the working principle of an ion thruster is shown in Figure 13. In the classical concept, ions are generated by electron bombardment, i.e. by collisions between propellant molecules and electrons injected in the ionization chamber. The ions are then accelerated by two grids between which a potential drop is applied. Since the expelled ions are positively charged, it is important to expel an equal number of negatively charged particles (electrons) in order to keep the spacecraft neutral. This is done by a component called neutralizer, which is basically the same as the component which injects the electrons in the ionization chamber.

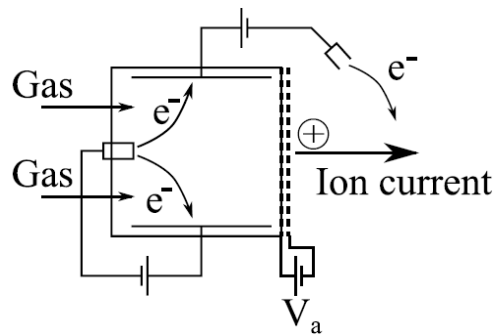


Figure 13: Schematic representation of a micro-ion thruster (from [6]).

As already mentioned in Chapter 1, a good propellant for an ion thruster is a fluid with high molecular mass and low ionization potential. Most of the current ion thrusters, either at the macro- or the micro-scale, use gaseous **Xenon** as propellant, which is one of the best available options according to these criteria.

A particular class of ion thrusters are Radio-Frequency electric thrusters, schematically shown in Figure 14. They are based on exactly the same working principle as ion thrusters, with the only difference that propellant is not ionized by electron bombardment, but by Radio

Frequency (RF) power provided by coils wrapped around the ionization chamber, creating an azimuthally oscillating electric field to generate the ions. Although they introduce some simplification due to the smaller number of required components (in particular, the internal electron generator is not necessary), RF thrusters are affected by a number of drawbacks when compared to electron bombardment ion engines: they are usually less efficient and require bulky electronics for the conversion from the power provided by the solar panels (typically DC) to the RF power required by the thruster coils. Xenon is still a common propellant choice for miniaturized Radio-Frequency thrusters, but **Iodine** is also a very typical alternative that allows for higher storage density and smaller tank volumes.

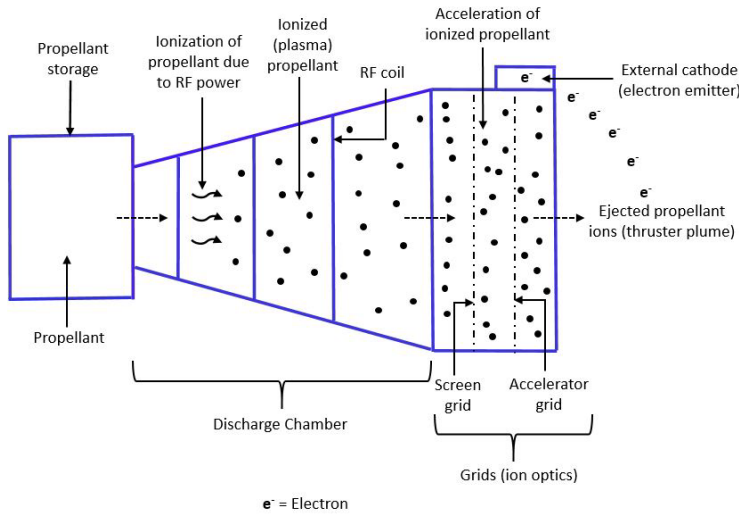


Figure 14: Working principle of a Radio-Frequency electric thruster (from [5]).

Ion thrusters have been among the first ones to be miniaturized for small satellites, especially as a potential solution for precision formation flying applications. Therefore, several micro-ion thrusters have been designed, built, and tested, often with a dedicated interface for CubeSats. Some of the available alternatives include:

- The Miniature Xenon Ion Thruster (**MiXI**) from JPL, which requires a power of 50 W to operate at a thrust of 1.4 mN and specific impulse of 3050 s. The power and volume characteristics of this system are not optimized for CubeSats, since it was developed before the rise of this small satellite format.
- The **NPT30-I2** gridded ion thruster developed by the company ThrustMe, using iodine as propellant and capable of delivering a thrust level in the range from 0.3 to 1.1 mN when using an input power in the range from 35 to 65 W.
- The dual system (ion thruster + resistojet) developed by the University of Tokyo, including two different thrusters sharing the same propellant (water). The ion thruster in this system has a limited specific impulse of 416 s due to the unconventional water propellant, but is capable of delivering a thrust level of approximately 0.25 mN at 45 W input power, in line with the performance of other existing micro-ion thrusters.
- The **μ NRIT-2.5**, a miniaturized RF thruster developed by Giessen University and Astrium in Germany. The thruster generates a thrust of 50 μ N with a power of 12.5 W at however a relatively low specific impulse (compared to other typical ion thrusters) of just 360 s.
- The 1-cm ion thruster (**BIT-1**) and 2.5-cm ion thruster (**BIT-3**, Figure 15) developed by Busek Co. The BIT-3 is designed specifically for a 3U or larger CubeSat format, and produces 0.95 mN of thrust with a power of 68 W and a specific impulse of 2300 s. The BIT-1 is a miniaturized version that operates at a smaller thrust level of 0.1 mN, thus requiring a reduced power of just 10 W.

- The Radio Frequency Thrusters **RFT** and **CAT** developed by Phase Four, based on the use of a permanent magnet and capable of operating with various possible propellants such as Xenon, Iodine, Argon, Krypton and even water. These thrusters are specifically designed for CubeSats and generate thrust in the order of a few mN with, however, a specific impulse not higher than 800 s.



Figure 15: The BIT-3 ion thruster produced by Busek Co. (from [8]).

2.7 Hall Effect thrusters

Also in Hall Effect thrusters (Figure 16), thrust is generated by first ionizing and then accelerating the propellant. However, in this case, a different acceleration mechanism is used, based on mutually perpendicular **electric** and **magnetic** fields applied to the ionization chamber.

As in ion thrusters, electrons are injected in the ionization chamber. As a consequence of the Hall effect, they start moving in a spiral trajectory with velocity perpendicular to both the magnetic field \mathbf{B} and the electric field \mathbf{E} . Ionization of the propellant, as usual, is obtained through collisions between these electrons and the propellant molecules, and propellant ions are then accelerated by the applied electric field. Therefore, no grids are needed in this case to accelerate the propellant, and they are replaced in practice by the applied magnetic field which, in a typical Hall Effect thruster, is radial.

Hall Effect thrusters are typically characterized by high specific impulse (although slightly lower than ion thrusters), high thrust density and design simplicity. Their main drawback, especially when used at the micro-scale, is the very low efficiency and, consequently, extremely high required input power. They typically use the same type of propellants as ion thrusters, such as **Xenon**, **Krypton**, **Iodine**, **Argon**.

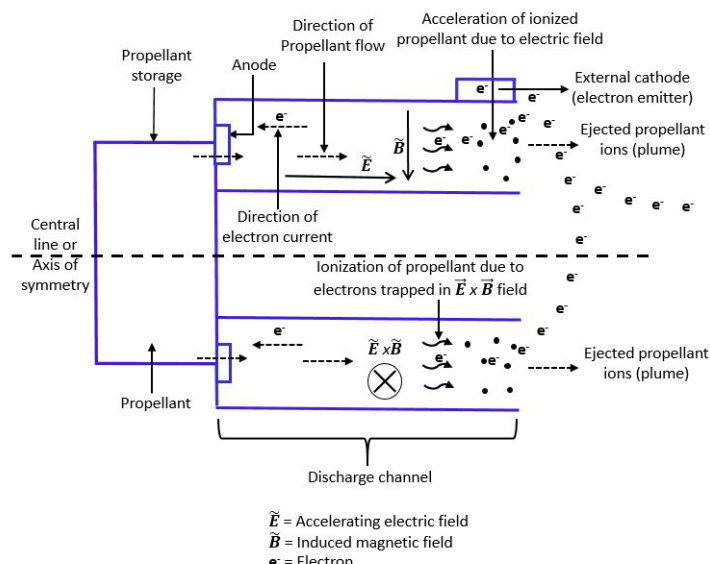


Figure 16: Working principle of a Hall effect thruster (from [5]).

Due to the mentioned down-scaling difficulties and high power requirements caused by the low efficiency, no Hall Effect thrusters are currently available at a scale that can be easily applied to small satellites such as CubeSats. As an example, the **BHT-200** thruster from Busek Co., working with Xenon as propellant, has been successfully demonstrated on the TacSat-2 microsatellite launched in 2006, but is characterized by a 200 W required input power to generate a thrust of 13 mN at a specific impulse of 1390 s, which makes it not suitable to the current power capabilities of typical CubeSats. Nevertheless, a version of the BHT-200 using Iodine as propellant is planned for use in the iSAT mission, a 12U CubeSat specifically intended for demonstration of this propulsion technology. Applicability of Hall Effect thrusters to small satellite missions is however expected to become more feasible in future, combined to the development of more efficient photovoltaic generators and, consequently, more performing electrical power generation systems.

2.8 Electrospray thrusters

Electrospray thrusters (Figure 17) are based on electrostatic acceleration of charged ions from a liquid propellant to produce thrust. The propellant is a conductive liquid and its surface is deformed by a strong electric field into a sharp cone-shaped meniscus called **Taylor Cone**; when a certain electric potential threshold is reached, ions are extracted from the cone and then accelerated by the same electric field used for their extraction. Both positive and negative ions are accelerated, thus there is no need for an additional neutralizer as in ion thrusters. The propellants used by electrospray thrusters are usually **ionic liquids**, characterized by a very small vapour pressure that allows for avoiding propellant pressurization. Additionally, ionic liquids do not require heating, have low operating voltage and high conductivity. Typical propellants include liquid metals such as **Cesium**, **Gallium** and **Indium**, or solutions of Formamide, Propylene Carbonate, water, Tri-Ethylene Glycol doped with Sodium Iodide or other ionic salts.

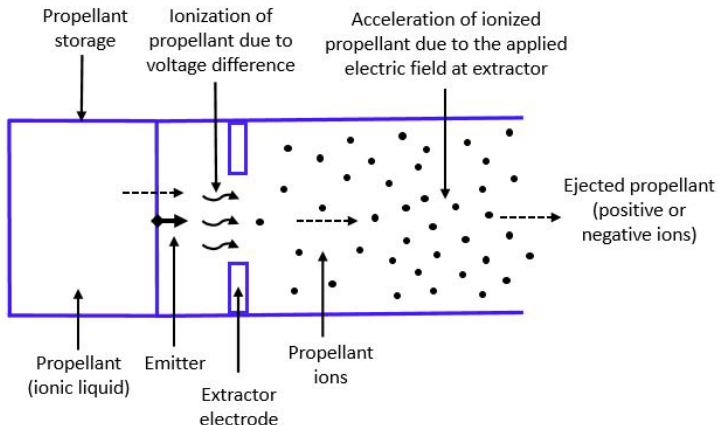


Figure 17: Working principle of an electrospray thruster (from [5]).

The ion acceleration principle in electrospray thrusters is exactly the same as ion thrusters; therefore, equations (1.7), (1.8), (1.9) and (1.10) still apply, and the applied electric field voltage plays a major role in defining the performance of the thruster.

An individual electrospray emitter normally operates at a power in the mW range and generates thrust in the order of micro-Newtons. However, by combining several emitters in an array, it is possible to obtain higher thrust levels at the cost of a higher required input power.

Several electrospray thrusters have been developed, or are currently under development, for small satellites. They include:

- The **BET-1mN** electrospray thruster from Busek Co., producing 0.7 mN thrust at 14 W input power and 800 s specific impulse, and the **BET-100** from the same company,

operating at a slightly lower thrust level of 0.1 mN, with 5.5 W input power and 1800 s specific impulse.

- The Scalable ion Electrospray Propulsion System (**S-iEPS**) developed by the Massachusetts Institute of Technology and flight demonstrated in the IMPACT CubeSat mission. The S-iEPS propulsion systems shown in Figure 18 are modular and consist of an 8-thrusters unit capable of providing 74 μ N of thrust at a specific impulse of 950 s.

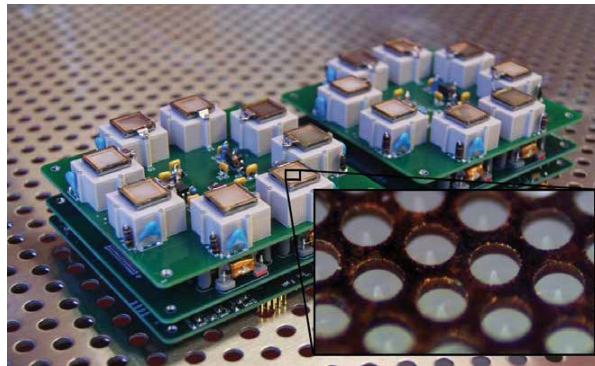


Figure 18: Eight-units versions of the S-iEPS electrospray thruster developed by MIT (from [6]).

2.9 Pulsed Plasma Thrusters

Pulsed Plasma Thrusters or PPT (Figure 19) operate by creating a pulsed, high-current discharge across the exposed surface of a solid propellant (usually Teflon). The arc discharge, usually generated in a pulsed way by a spark plug, ablates the propellant material generating ionized molecules which are then accelerated. The current pulse usually has a duration of a few microseconds and is driven by a capacitor charged and discharged approximately once per second. A spring mechanism ensures that there is always a propellant surface which can be ablated close to the spark plug.

The ablated propellant ions flow in a chamber between an anode and a cathode and, being conductive, close the electrical circuit generated by the voltage provided by a Power Processing Unit (PPU), thus allowing current to flow from the anode to the cathode. This current, in turn, produces a self-induced magnetic field (perpendicular to the plane on which Figure 19 is drawn), and the propellant ions are accelerated by a **Lorentz force** perpendicular to both the electric and the magnetic fields.

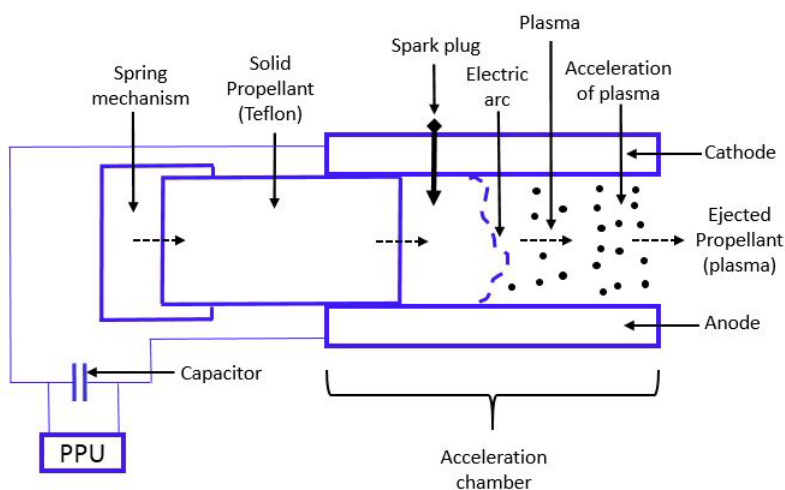


Figure 19: Working principle of a Pulsed Plasma Thruster (from [5]).

The main advantages of Pulsed Plasma Thrusters are their ability to provide very small impulse bits for precision maneuvers, simplicity due to the relatively small number of

components, possibility of using a wide range of propellants (not only solid but also in the liquid state) and adjusting the thrust level by varying the pulse frequency, fast response time to commands. However, they also suffer from major drawbacks such as rapid erosion of the electrodes, presence of non-ionized macro-particles in the exhaust plume due to non-uniform ablation, relatively high dry mass due to the bulky electronics required for their operation, and very low efficiency (typically in the 10-15% range).

Although no Pulsed Plasma Thrusters have been demonstrated in orbit at the present day, a significant amount of research on PPTs for CubeSats has been carried out in recent years. Some of the systems already developed or under development include:

- The Micro-Pulsed Plasma Thruster (**μPPT**) developed by the Austrian Institute of Technology and operating with Teflon. It is capable of a thrust of 20 μN at a specific impulse of 900 s.
- The **PPTCUP** system developed by Mars Space Ltd. (Figure 20), capable of a thrust of 40 μN at a specific impulse of 600 s with input power of 2.7 W.
- The **μPPT** thruster developed by Busek for the FalconSat-3 microsatellite (0.5 mN thrust, 2 W input power, 700 s specific impulse), and the **BmP-200** from the same company (0.14 mN thrust, 3 W input power, 536 s specific impulse).

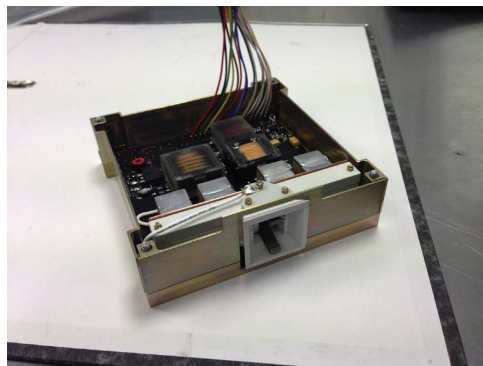


Figure 20: The PPTCUP Pulsed Plasma Thruster unit produced by Mars Space Ltd. (from [8]).

A particular class of PPTs are the so-called **Vacuum Arc Thrusters**, which are based on exactly the same principle, with the only difference that propellant ablation is obtained by a vacuum arc instead of a spark plug. In this case the ions to be accelerated are ablated directly from the cathode material (which is therefore, as a matter of fact, the propellant itself), allowing for higher efficiency. Differently to PPTs, one model of Vacuum Arc Thruster has been actually demonstrated in space: the Micro Cathode Arc Thruster (**μCAT**) developed by George Washington University, four units of which have been successfully used on-board the BRICSat-P, a 1.5U CubeSat, to detumble the satellite after deployment.

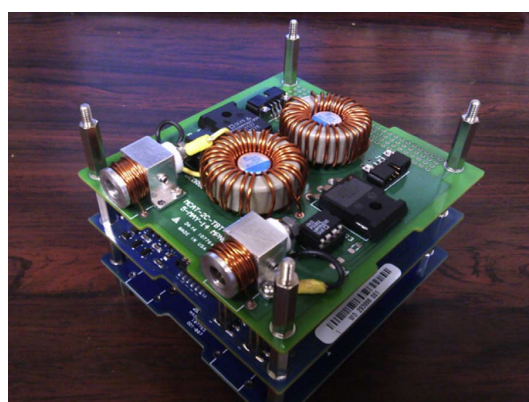


Figure 21: The μCAT Vacuum Arc Thruster developed by the George Washington University (from [8]).

2.10 General overview and conclusions

A complete overview of all micro-propulsion systems identified in the state-of-the-art study reported in this Chapter is provided in Tables 1 and 2. These tables include not only the systems that have already been demonstrated in space, but also those which are still at a prototype or engineering model stage, but already at a sufficient level of development to make it possible to define in a clear way their main performance characteristics.

For each system in the tables, the company (or institution) which has developed it is indicated, as well as the propellant(s) used by the system (when this information is available). The design/performance parameters available for all systems are the nominal **thrust level**, nominal **specific impulse** and the **dry mass** (i.e., complete mass of the whole system without propellant). The **input power** and **thrust/power ratio** are provided only for electric propulsion options and for resistojet, thus only for those systems where the power is used directly for heating the propellant and/or accelerating it. *Note: this does not mean that the other types of micro-propulsion systems (cold gas, mono-propellant, bi-propellant, solid propellant) do not require any power to be operated. They will always require a certain amount of power to operate active fluid control elements (such as valves or igniters, when present) or for active thermal control of the propellant or the catalyst, if needed. However, this power will not go directly in the acceleration process of the propellant and, therefore, will not play a direct role in the generation of thrust.*

When a parameter for a certain system is not available or could not be found in literature, that cell is left empty in the tables.

The plots from Figure 22 to Figure 29 graphically summarize the information given in Tables 1 and 2. They help to identify specific trends in the performance of different types of micro-propulsion and will be widely used for the analysis of small satellite applications in the next Chapter. In some of the plots, the performance limits of each type of micro-propulsion system are roughly identified and shown by means of coloured oval areas. Note that some “outliers” in Tables 1 and 2, with clearly different performance than the other systems in the same category (due for example to the use of an unconventional propellant, or a slightly different working principle), have been left out of the plots. The main conclusions that can be drawn by analysing the plots are discussed in detail in the following.

Thrust – Specific Impulse

The chart in Figure 22 shows very clearly defined and relatively limited performance areas for each type of micro-propulsion system under consideration. This means that a certain micro-propulsion system type can be used only for a limited range of thrust-specific impulse combinations; therefore, the propulsion system choice becomes rather obvious in applications characterized by specific requirements in terms of these two performance parameters.

All pure electric propulsion options can be found in the region of high specific impulse (typically 500 s or higher) and low thrust (typically a few mN or lower, with the only notable exception of Hall Effect and ion thrusters). Cold gas and resistojets allow for a wider range of thrust levels (from 0.1 mN to 0.1 N) but are typically limited to specific impulse values lower than 100 s. Chemical propulsion options are the only ones which allow for a thrust level higher than 0.1 N, but are confined to a narrow specific impulse range between 200 and 300 s.

Thrust – Power

As indirectly suggested by equation (1.10) in Chapter 2, the input power of an ion thruster is proportional, at least in a first simplified approximation, to the jet velocity squared v_e^2 . Looking at equation (1.7), this means that the input power is proportional to the grid voltage V and thus, from equation (1.8), the thrust is proportional to the input power squared. In a logarithmic thrust-power chart (like the one in Figure 23) this translates into a “10/100” slope: when the power is increased by one order of magnitude (factor 10), the thrust increases by two orders of magnitude (factor 100). Notably, this trend is followed with good fitting accuracy by the highlighted areas in Figure 23, not only for ion thrusters but also for other types of electric propulsion and even for resistojets. However, the resistojet region is located in a lower area of the chart, meaning that they require lower input power than other systems

to produce the same amount of thrust, and are therefore characterized by a higher thrust/power ratio.

Specific Impulse - Power

Differently to the thrust-power case, the specific impulse-power chart (Figure 24) is deviating from the theoretical expectations. When looking at equation (1.9) in the previous Chapter, and after combining it with equations (1.10) and (1.7) similarly to what done above for the thrust, the specific impulse would be expected to be proportional to the square root of the power or, in other words, a “100/10” slope in the logarithmic chart of Figure 24. However, in the figure, this trend seems to be followed only by electrospray thrusters, with most of the other propulsion types showing very weak or even no clear relationship between specific impulse and power. Although the number of data points in the chart and their distribution are not sufficient to draw any definitive conclusions, it is likely that a certain type of electric propulsion is preferred to always work in a given specific impulse range independently on the amount of input power required. This is probably a consequence of general efficiency considerations given that, in electric propulsion, the thruster efficiency is usually a direct function of the specific impulse and it is typically possible to find a specific impulse value for which efficiency is maximum.

Thrust/Power Ratio

When analyzing the thrust/power ratio as a function of the thrust (Figure 25) and the specific impulse (Figure 26), some very clear trends become apparent.

As already anticipated by the thrust-power chart, resistojets offer a significantly higher thrust/power ratio than any other systems, typically in the range 0.2-1 mN/W. Combined with their typical thrust range (0.2-20 mN), this shows that resistojets are an optimal solution when a thrust in the order of a few mN is required with an available input power in the order of a few W (as it typically happens in CubeSats or other similar small satellites).

The second best option in terms of thrust/power ratio are Hall Effect thrusters (0.03-0.1 mN/W), but they are typically characterized by a thrust level in the order of 6 mN or higher which, combined to their thrust/power ratio range of values, leads to an input power of 100 W or higher, which is typically not compatible to the requirements of small satellites.

All other options approximately cover the region below 0.05 mN/W, with just a few exceptions for some specific products.

Dry Mass

The dry mass of all systems for which this information is available is shown as a function of the thrust (Figure 27), specific impulse (Figure 28) and input power (Figure 29). In these figures, however, only the points related to individual systems are shown, not highlighting the generic regions covered by each type of micro-propulsion system due to the very large overlapping and not easily identifiable areas to which each micro-propulsion type belongs.

Nevertheless, some interesting trends can still be identified. Looking at the dry mass as a function of thrust, a clearly increasing trend (higher dry mass with increasing thrust) can be observed for thrust levels up to 10 mN, while dry mass values tend to stay approximately constant for thrust levels higher than 10 mN. This can be explained by the fact that only cold gas or chemical propulsion systems are present in the thrust range of 10 mN or higher (with the only exception of Hall Effect thrusters). These systems are all based on accelerating the propellant in a nozzle: by combining equations (1.1), (1.4) and (1.5) from previous Chapter, it can be seen that the thrust is proportional to chamber pressure and nozzle throat area; however, in micro-propulsion systems, the chamber pressure is typically low and the nozzle is normally very small, meaning that changing their values to modify the thrust level does not affect the mass of the whole system in a significant way.

Conversely, no clear trends can be observed in the dry mass as a function of the specific impulse. A slightly increasing trend seems to be present in the dry mass as a function of the input power, which can be explained by observing that systems requiring a higher power will typically also require more complex and heavier power management and conditioning components.

Table 1: Main characteristics of state-of-the-art micro-propulsion systems (part 1).

Type	Company/Institution	Name	Propellant	Thrust (mN)	Power (W)	T/P (mN/W)	Dry mass (g)	Isp (s)
Cold Gas	SSTL	SNAP 1	Liq. Butane	46				43
	UTIAS-SFL	CNAPS	SF6	50			260	45
	SFL	NANOPS	SF6	35			480	46,7
	Microspace Rapid	POPSAT-HIP1	Argon	1				43
	GOM Space	MEMS Cold gas	Liq. Butane	1			300	50
	GOM Space	NanoProp 6DOF	Liq. Butane	1			682	50
	GOM Space	NanoProp 2000	Liq. Butane	1			380	50
	GOM Space	NanoProp CGP3	Liq. Butane	1			300	60
	GOM Space	NanoProp 6U	Liq. Butane	1			770	60
	VACCO	CPOD	R134a	25			770	40
	VACCO	MEPSI MiPS	Isobutane	53			456	65
	VACCO	MarCO MiPS	R236fa	25				
	VACCO	NEA Scout MiPS	R236fa	25			1263	39,8
	VACCO	MiPS	R134a	10			625	40
	VACCO	AFRL PUC	SO2	4,5			835	46
	VACCO	Palomar MiPS	Isobutane	35			890	50,1
	VACCO	CuSP	R134a, R236fa	25			513	
	VACCO	Standard MiPS	R236fa	25			1144	40
	MOOG	058 E143	Nitrogen	10				60
	Marotta Controls	SV14	Nitrogen	10				70
	Advanced Space Technologies	CGT	Nitrogen	42				69
	Nammo	SVT01	Nitrogen	10				72
	Aerospace Co.	MEPSI	Xenon	0,1			188	30
	Lightsey Space Research	BioSentinel	R236fa	40			1080	40,7
	NanoSpace	CubeProp	-----	0,1			115	75
	Univ. of Toronto	NANOPS	-----	50				45
	TNO-TU Delft	T3μPS	Nitrogen	6				68
	Univ. of Texas	Bevo-2	R236fa	110,8			290	65
	Univ. of Texas	3D Printed Cold Gas	R236fa	35				55,4
	Univ. of Texas	Custom Cold Gas	R236fa	110			290	64
Mono-propellant	Aerojet Rocketdyne	GPIM	AF-M315E	400				235
	Aerojet Rocketdyne	MPS-120	Hydrazine	1000			1300	225
	Aerojet Rocketdyne	MPS-130	AF-M315E	1000			1300	240
	ECAPS	HPGP	LMP-103S	1000				231
	Busek	BGT-X1	AF-M315E	100				214
	Busek	BGT-X5	AF-M315E	500			1240	220
	VACCO	ADN MiPS	ADN	100			900	258
	ECAPS	1N HPGP	LMP-103S	1000				220
Bi-propellant	NanoAvionics	EPSS C1K	ADN	100				210
	Hyperion/Dawn Aerospace	PM400	Nitrous Oxide + Propene	1000			1400	285
	Hyperion/Dawn Aerospace	PM200	Nitrous Oxide + Propene	500			1100	285
	Benchmark Space Systems	Peregrine	H2O2 + NHMF	1000			1839	270
	Tethers Unlimited	HYDROS-C	Liquid water (electrolyzed)	1200			2200	310
Resistojet	SSTL	LPR	Xenon	18	30	0,60	200	73
	VACCO	PUC	SO2, R134a, R236fa	5	15	0,33	450	70
	VACCO	CHIPS	R134a	31	25	1,24	760	76
	Busek	AMR	R134a	10	15	0,67	1250	150
	Busek	Microresistojet	Ammonia	10	9	1,11	1250	150
	University of Tokyo	AQUARIUS (DeltaV)	Water	4	18,18	0,22	800	70
	University of Tokyo	AQUARIUS (RCS)	Water	1	4,55	0,22	800	70
	Purdue University	FEMTA	Water	0,23	1	0,23		80
	Hong Kong University	Low-Power VLM	Water	1,014	3,6	0,28		86
	NanoSpace	CubeSat MEMS	Butane	1	2	0,50	295	92
	Aurora Propulsion Technologies	ARM-A	Water	2,3	11	0,21	230	100
	CUA	NEA Scout	R134a, R236fa	25			1180	66
	EDB Fakel	Gas resistojet	Xenon	7,85	10,7	0,73	220	42,5
	SteamJet	TunaCan Thruster	Water	6	20	0,30	540	172
	TU Delft	VLM	Water	1,52	5,25	0,29	310	94,9
	TU Delft	LPM	Water	1,14	4,51	0,25	280	88,1
Solid propellant	Univ. of Southampton	STAR	Argon	12,8	12,75	1,00		69
	Univ. of Southern CA	FMMR	Water	1,7	4,1	0,41		79,2
	Aerospace Co.	30s	-----	37000				187
	Orbital ATK	STAR 4G	Al + Ammonium perchlorate	13000			508	269,4
DSSP	CAPS-3	HIPEP-501A						245
	CDM-1	AP/HTPB		76000			460	226

Table 2: Main characteristics of state-of-the-art micro-propulsion systems (part 2).

Ion thrusters	Busek	BIT-1	Xenon, Iodine	0,105	10	0,01	50	2250
	Busek	BIT-3	Xenon, Iodine	0,955	68	0,01	1400	2300
	Airbus	RIT- μ X	Xenon	0,275	50	0,01	440	3000
	Airbus	RIT 10 EVO	Xenon	5	145	0,03		1900
	Avant Space	GT-50	Xenon	6	210	0,03		2000
	Qinetiq	T5 Mk 5 (GOCE)	----	10,5	330	0,03		1750
	Qinetiq	T5 Mk 6	----	15,5	475	0,03	2000	2600
	University of California	MiXi	Xenon	1,2	29	0,04		2810
	Astrium	μ NRIT-2.5	Xenon	0,5	31,2	0,02	210	2609
	Mars Space	Mini RF ion engine	Xenon	0,85	19	0,04	300	2500
	ThrustMe	NPT30-I2	Iodine	0,7	50	0,01	1200	2400
	JPL	MiXi	Xenon	1,4	50	0,03	200	3050
Hall thrusters	Busek	BHT-200	Xenon, Iodine, Krypton	13	200	0,07	980	1390
	Busek	BHT-600	Xenon, Iodine, Krypton	48,5	550	0,09	2600	1500
	Sitael	HT 100	Xenon, Krypton	12	235	0,05	650	1300
	Sitael	HT 400	Xenon	35	625	0,06	900	1850
	MIT	MHT-9	Xenon	12,3	347	0,04	1000	1706
	EDB Fakel	SPT-50M	Xenon	16,4	262,5	0,06	1320	1065
	EDB Fakel	SPT-70	Xenon	39	670	0,06	1500	1470
	EDB Fakel	PlaS-34	Xenon	22	230	0,10	970	1300
	EDB Fakel	PlaS-40	Xenon, Krypton	40	415	0,10	1200	1880
	EDB Fakel	PlaS-55	Xenon	72	800	0,09	2500	1950
	ExoTerra	Halo	Xenon, Krypton	18,5	262,5	0,07	670	1125
	Rafael	IHET-300 (R-400EPS)	Xenon	15	425	0,04	1600	1300
	SETS	ST25	Xenon, Krypton	8	170	0,05	950	1200
	SETS	ST40	Xenon, Argon, Krypton	21	425	0,05	1100	1850
	UTIAS-SFL	CHT	Xenon, Argon	6,2	200	0,03		1139
Electrospray	MIT	S-iEPS	Ionic liquid	0,074	1,5	0,05	100	950
	Accion Systems	Tile-2	Ionic liquid	0,04	4	0,01		1650
	Accion Systems	Tile-3	Ionic liquid	0,45	20	0,02		1650
	Accion Systems	IMPACT	----	0,06	1,5	0,04		1200
	Accion Systems	MAX-1	----	0,12	1,6	0,08		2000
	Busek	BET-1mN	Ionic liquid	0,7	14	0,05	1150	800
	Busek	BET-100	Ionic liquid	0,1	5,5	0,02	540	1800
	Enpulsion	IFM Nano	Indium	0,35	40	0,01	670	4000
	Enpulsion	IFM Nano SE	Indium	0,35	40	0,01	1230	4000
	Enpulsion	Nano	Indium	0,18	24	0,01	680	4000
	Enpulsion	Nano R3	Indium	0,18	24	0,01	1200	4000
	Enpulsion	Nano IR3	Indium	0,255	26,5	0,01	1200	2750
	Enpulsion	Micro R3	Indium	0,775	75	0,01	2600	3750
	Fotec GmbH	14-needle FEEP	----	0,5005			700	4000
	Morpheus Space	NanoFEEP	Gallium	0,0705	9,7	0,01	280	5550
Pulsed Plasma Thruster	Mars Space	PPTCUP	PTFE	0,04	2,7	0,01	280	600
	Mars Space	NanoPPT	PTFE		6,5			640
	Primex Aerospace	EO-1 PPT	PTFE	0,14	12,5	0,01		1150
	Busek	MPACS	PTFE	0,144	10	0,01	550	830
	Busek	BmP-220	PTFE	0,14	3	0,05	500	536
	Busek	μ PPT	PTFE	0,5	2	0,25	550	700
	Austrian Inst. Of Technology	μ PPT	PTFE	0,02	2,25	0,01	25	900
	Fotec GmbH	PPT	PTFE	0,01	1	0,01	300	900
	Fotec GmbH	μ PPT	PTFE	0,006			300	1100
Vacuum Arc Thruster	George Washington Univ.	μ CAT	Nickel	0,00255	0,1	0,03	200	2750
	Univ. of Illinois	μ BLT	Aluminum	0,054	4	0,01	150	2000
	Wurzburg University	UWE4	Titanium, Tungsten	0,002	0,5	0,00		900
Radio-Frequency Electric Thrusters	Phase Four	RFT	Xenon	2,77	50	0,06	1000	498
	Phase Four	CAT	Xenon, Iodine, Argon, Krypton	1	5	0,20	1000	800
	ArianeGroup	RIT μ X	Xenon	0,5	50	0,01	440	300
	T4 Innovation	Regulus-A 1.5U	Xenon, Iodine	0,55	50	0,01		550
	Astrium	μ NRIT-2.5	----	0,05	12,5	0,00	210	360

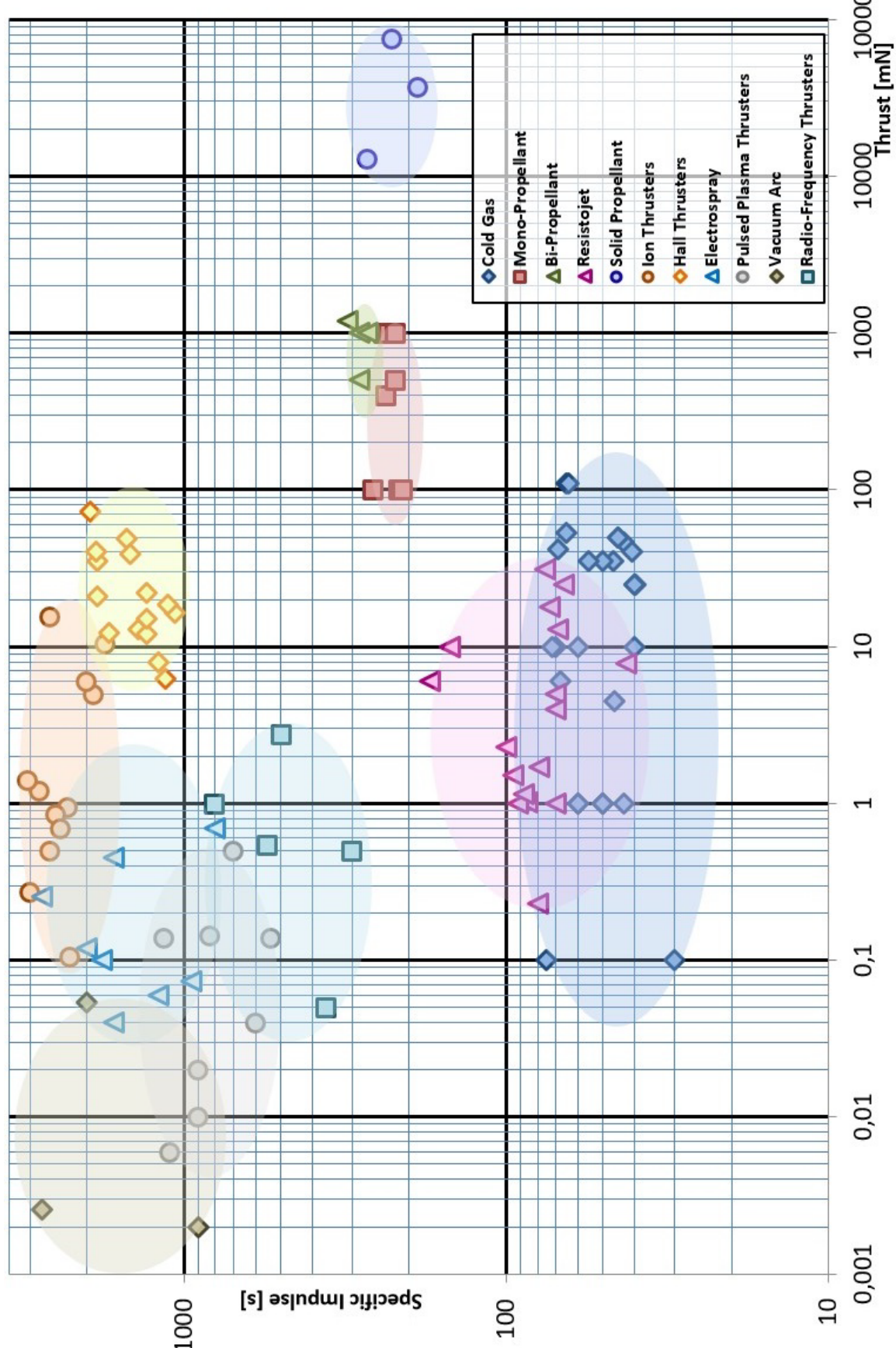


Figure 22: State-of-the-art micro-propulsion systems (thrust-specific impulse chart).

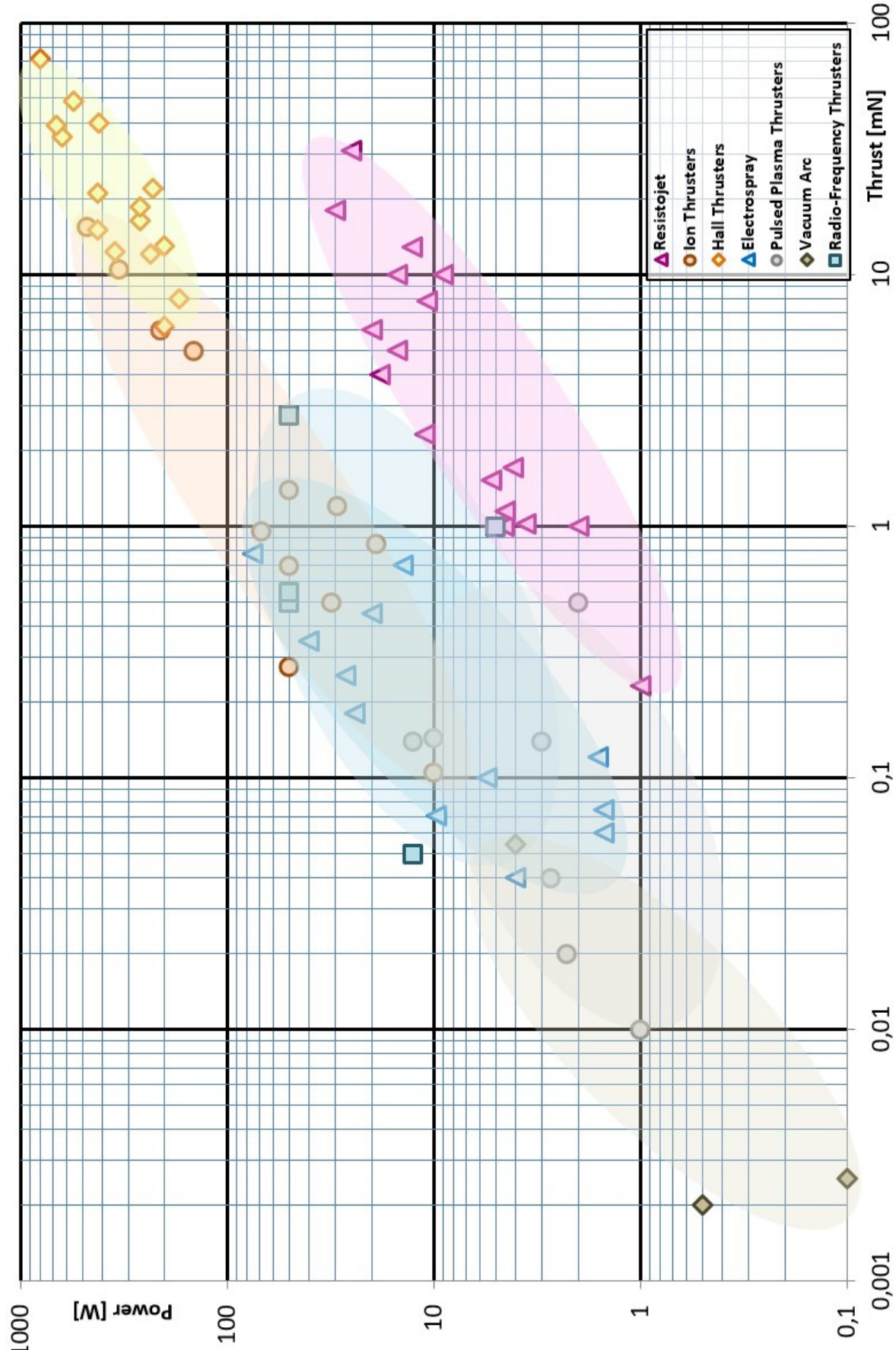


Figure 23: State-of-the-art micro-propulsion systems (thrust-power chart).

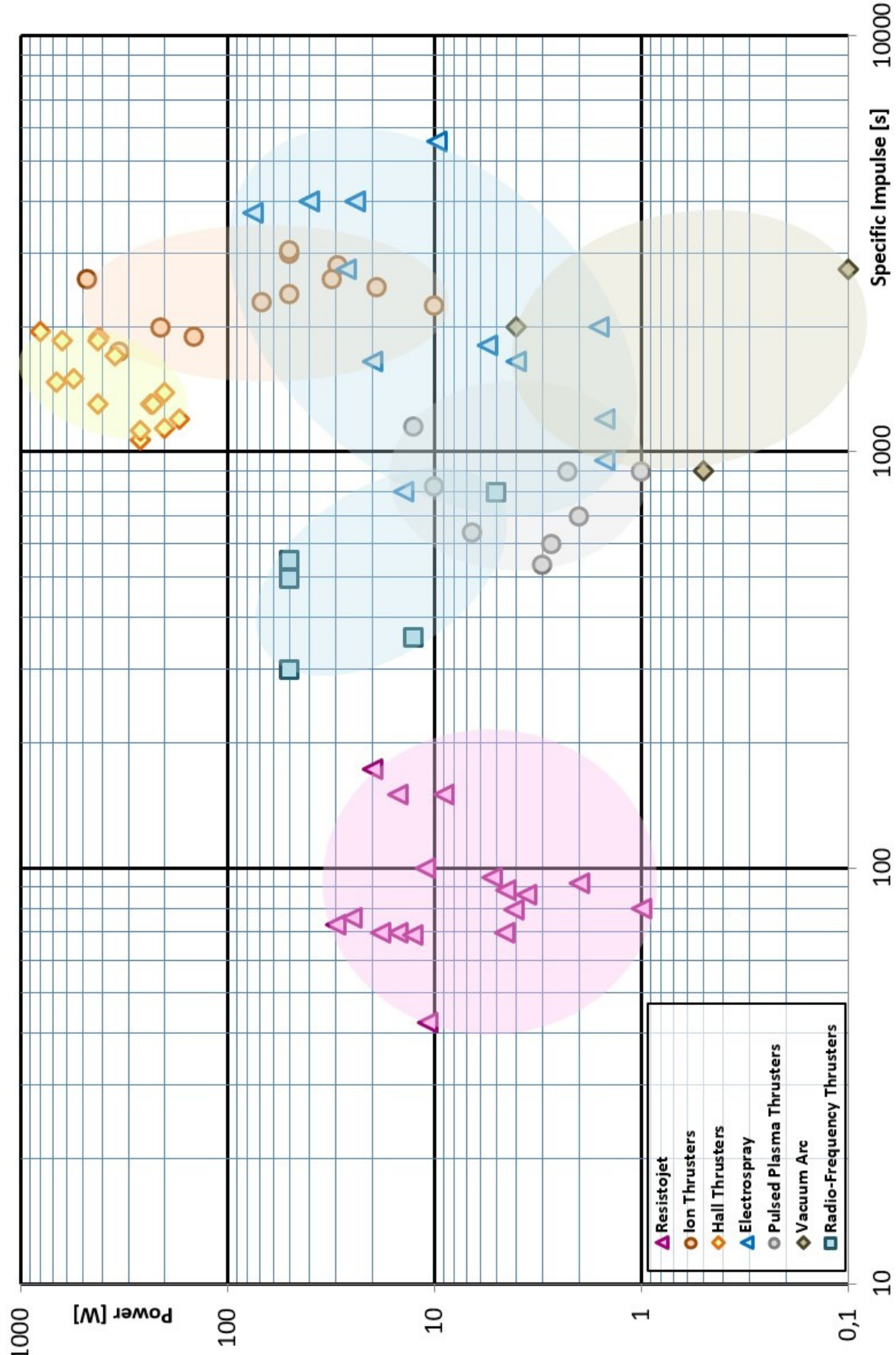


Figure 24: State-of-the-art micro-propulsion systems (specific impulse-power chart).

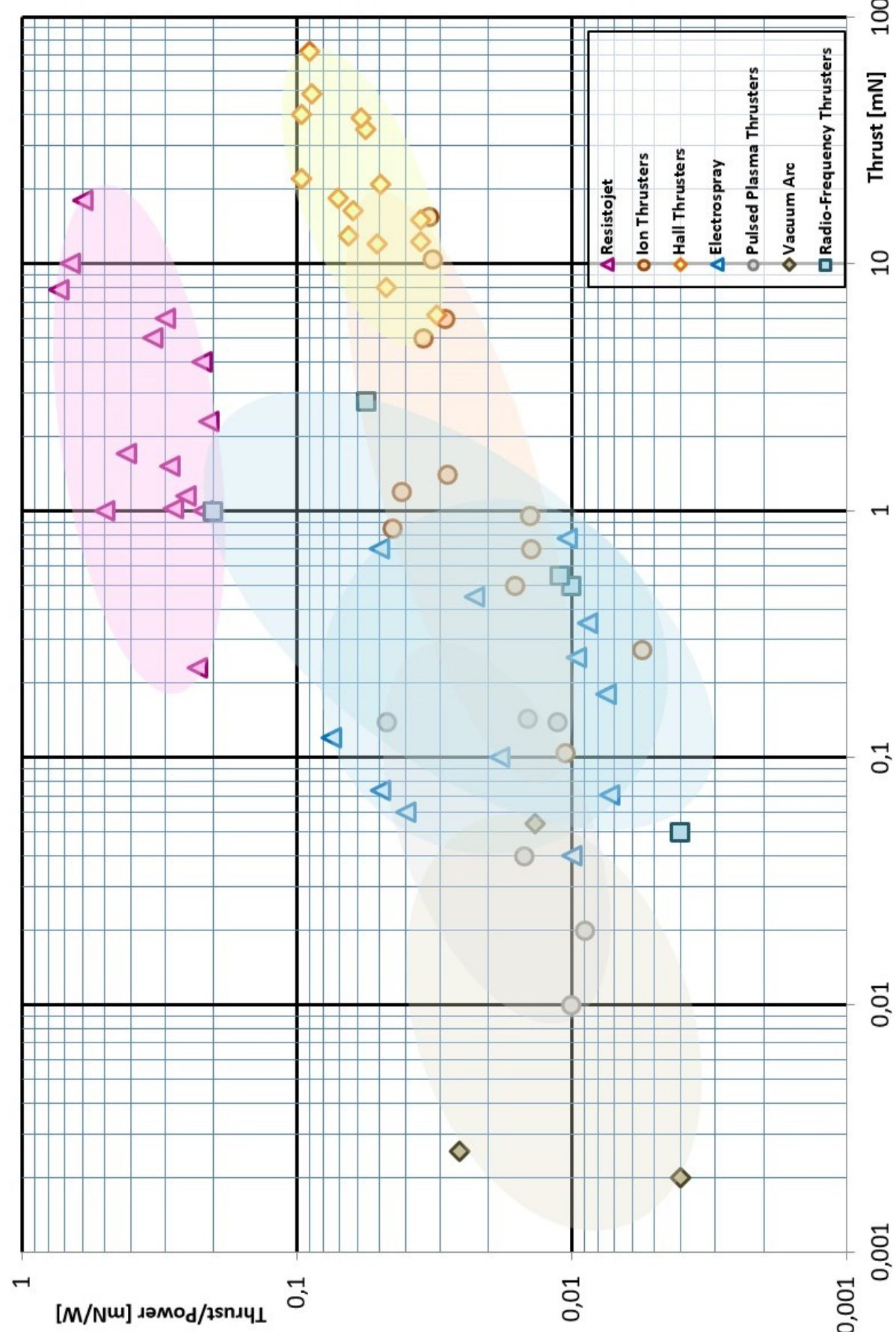


Figure 25: State-of-the-art micro-propulsion systems (thrust-thrust/power ratio chart).

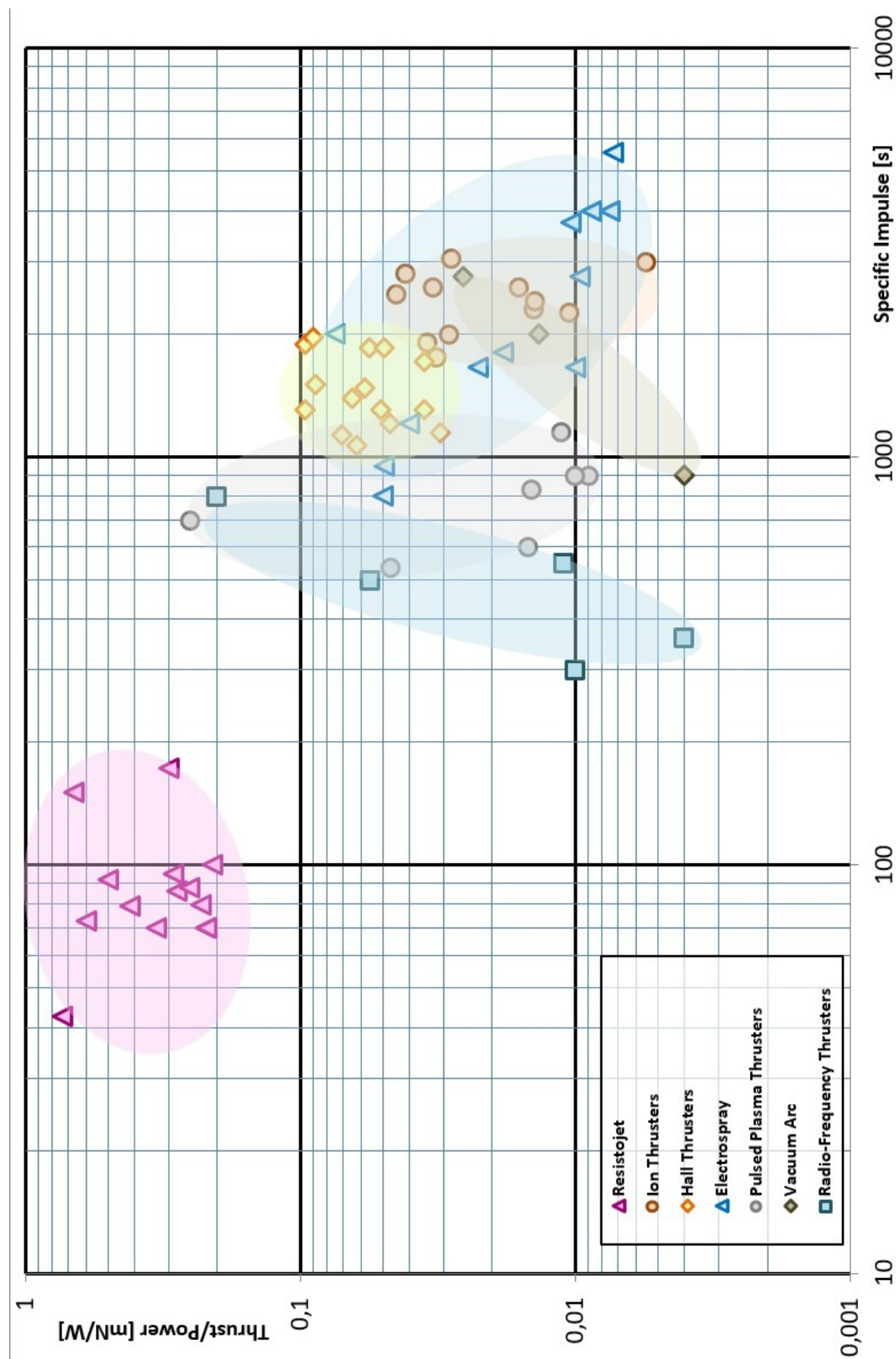


Figure 26: State-of-the-art micro-propulsion systems (spec.impulse-thrust/power ratio).

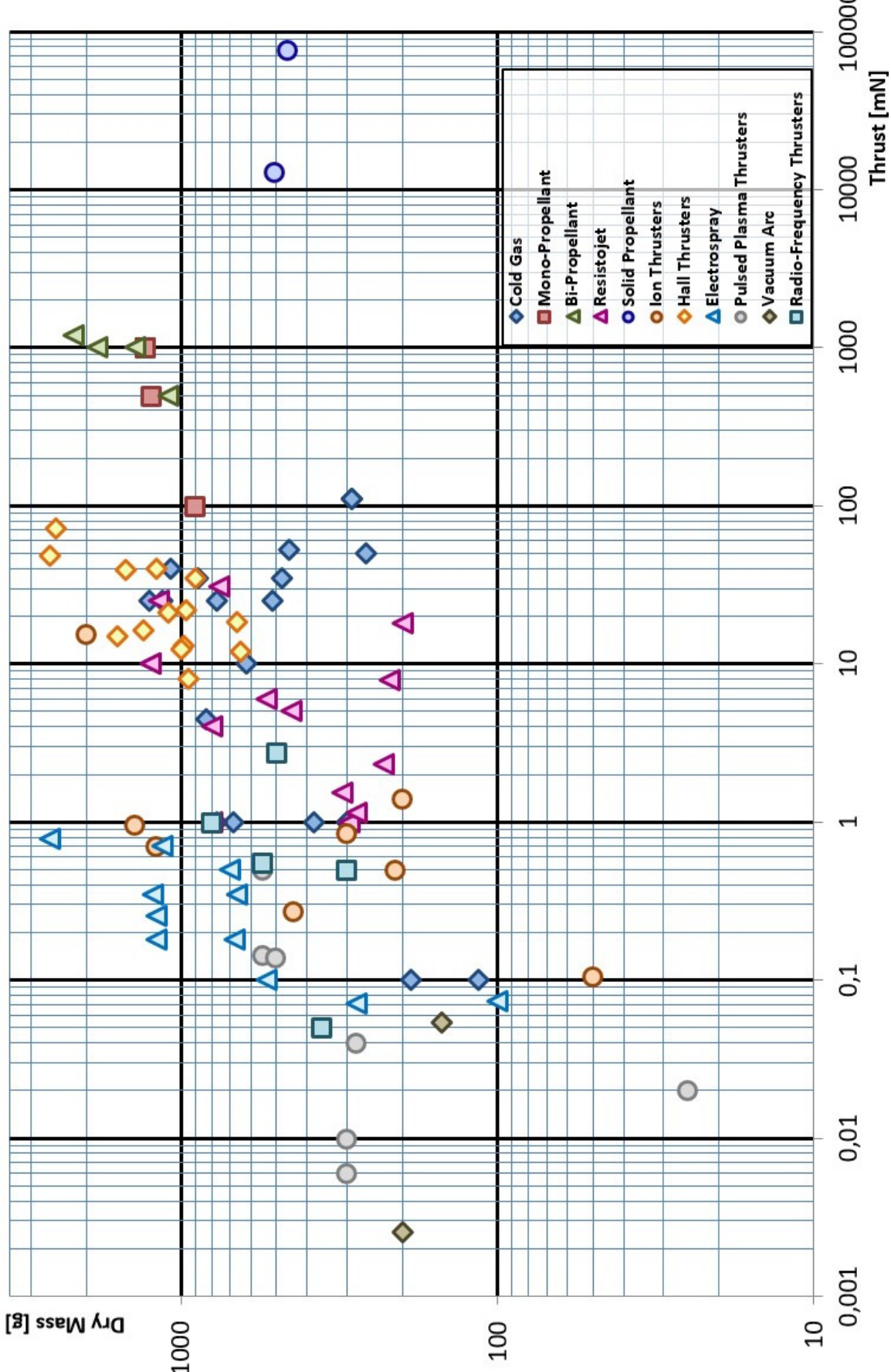


Figure 27: State-of-the-art micro-propulsion systems (thrust-dry mass chart).

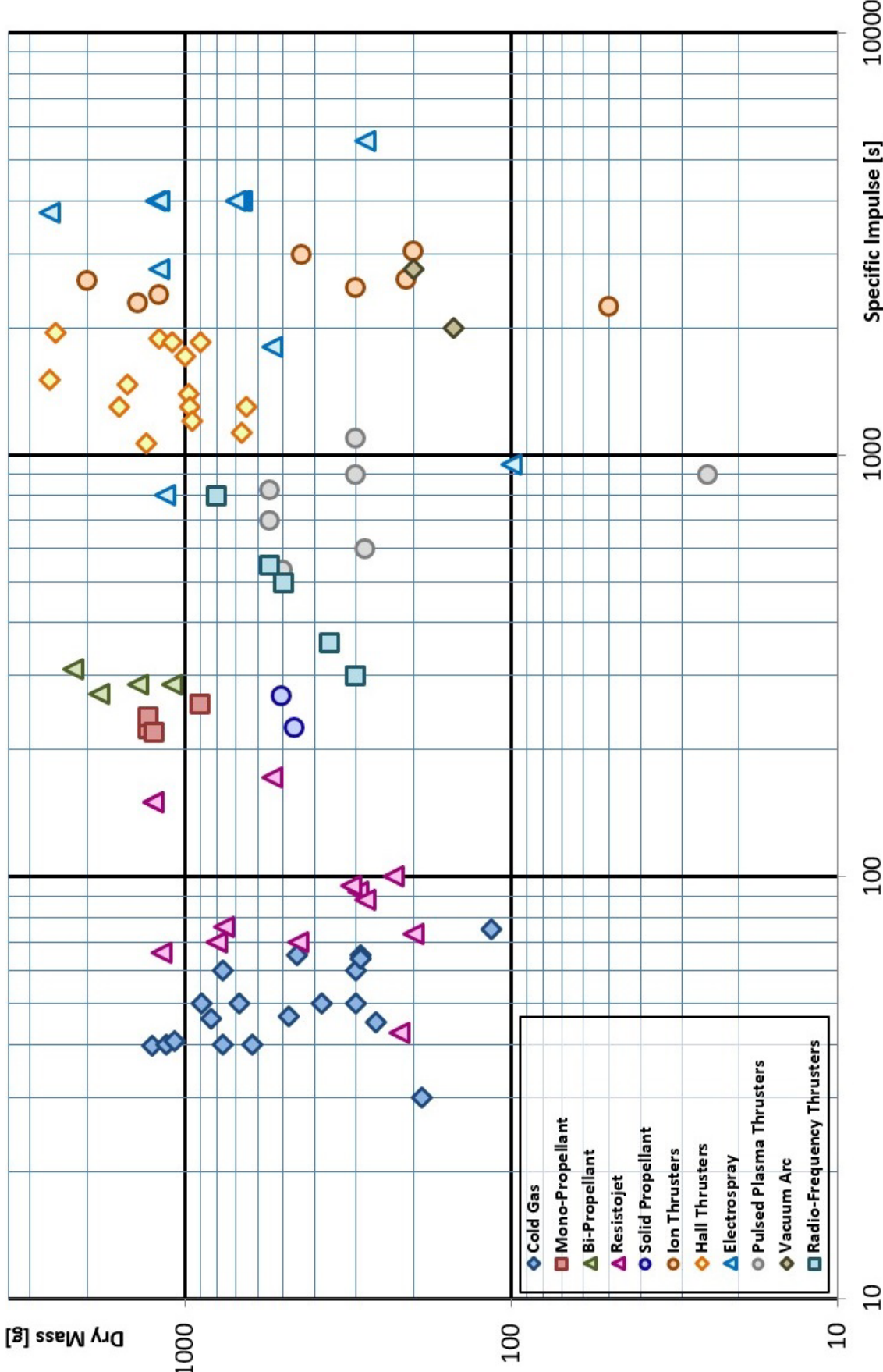


Figure 28: State-of-the-art micro-propulsion systems (specific impulse-dry mass chart).

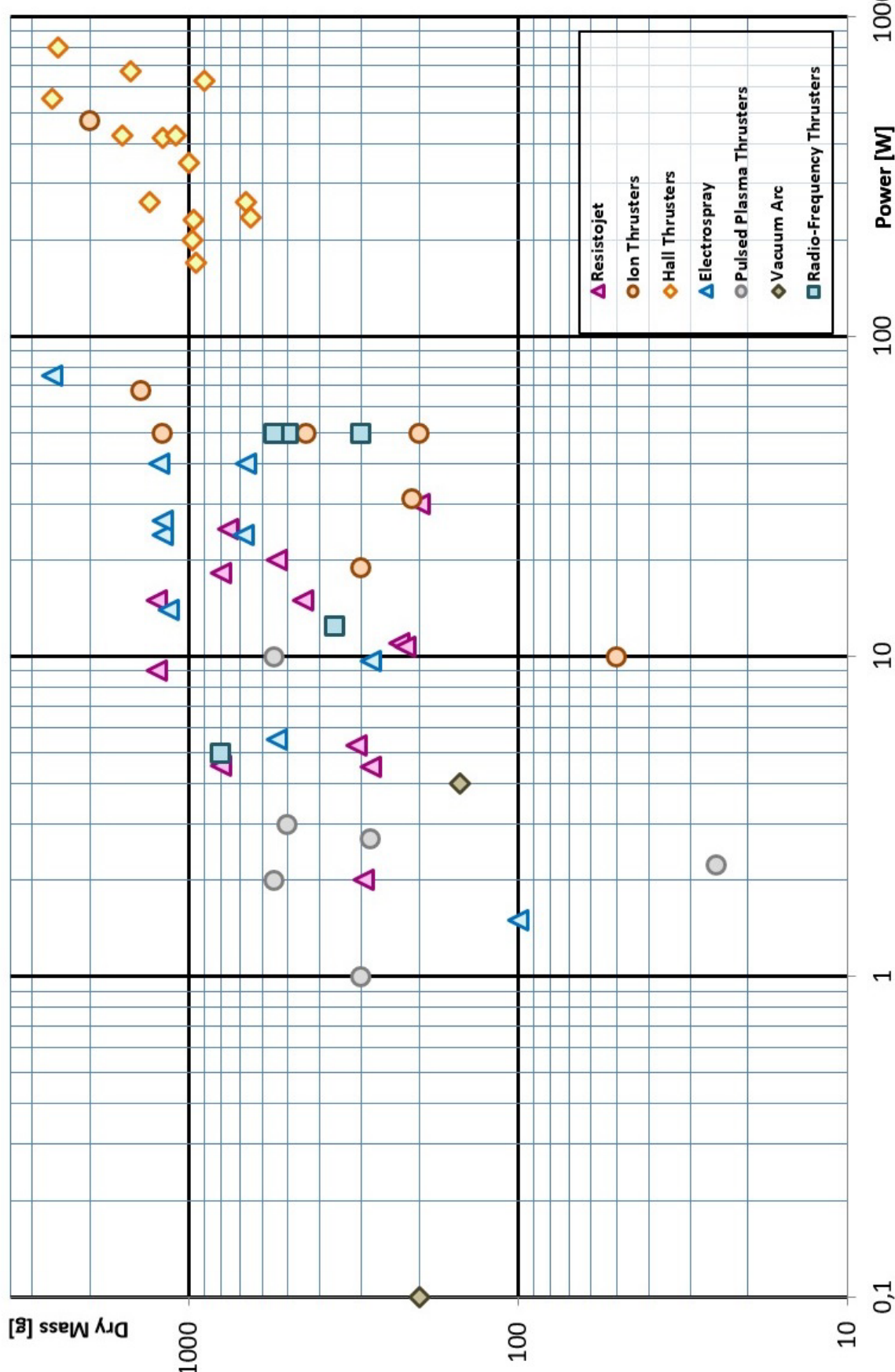


Figure 29: State-of-the-art micro-propulsion systems (power-dry mass chart).

3 – Applications to Small Satellites

In the following, the micro-propulsion state-of-the-art information provided in the previous Chapter will be used to define, in a systematic way, which types of micro-propulsion are better suitable to some specific small satellite applications.

As explained in the following section, four different small satellite formats have been considered for the study, as well as four different applications representative of the most typical ones for this class of satellites. The results show in a very clear way that there is no “perfect” micro-propulsion system, but just preferred option(s) that vary depending on the characteristics and requirements of the specific application.

3.1 Boundaries of the study: applications and small satellite formats considered

The study has been conducted considering four different small satellite formats, listed in the following with, in **bold**, the abbreviation that will be used for them throughout this whole Chapter:

- **3p**: 3-units PocketQube (approximately 5x5x5 cm unit standard), 1x3 units shape
- **1U**: 1-unit CubeSat (approximately 10x10x10 cm unit standard)
- **3U**: 3-units CubeSat, 1x3 units shape
- **12U**: 12-units CubeSat, 4x3 units shape

The choice of these specific formats is justified as follows. The CubeSat standard is the most widely used at the present day for small spacecraft. A large majority of the current CubeSats are designed according to the **3U** format, which is usually deemed sufficient for housing all subsystems and components of the satellite (especially for Low Earth Orbit missions) and is also the format for which most of the current deployers and launch opportunities are tailored. The **1U** is the original CubeSat format, not used very often at the present day but still useful for comparison to the other formats. The **12U** is the most typical format considered as of today for missions beyond Low Earth Orbit (such as Lunar or interplanetary CubeSats) and, more in general, for CubeSats where larger and more performing instrumentation is needed. Finally, the **3p** format reflects the most recent developments in further satellite miniaturization, based on the use of the PocketQube standard with eight times smaller units (in volume) than CubeSat ones.

The simplified geometries considered for the current study are shown in Figure 30, while the data used for the analysis are given, for each of the considered formats, in Table 3. These data are representative of the typical mass, size and power levels of the given small satellite formats; note, in particular, that mass and power are taken from historical information on the same satellite format and don't exactly scale with the spacecraft size. The moments of inertia have been calculated considering the simplifying assumption of uniformly distributed mass in a fully-parallelepiped shaped spacecraft.

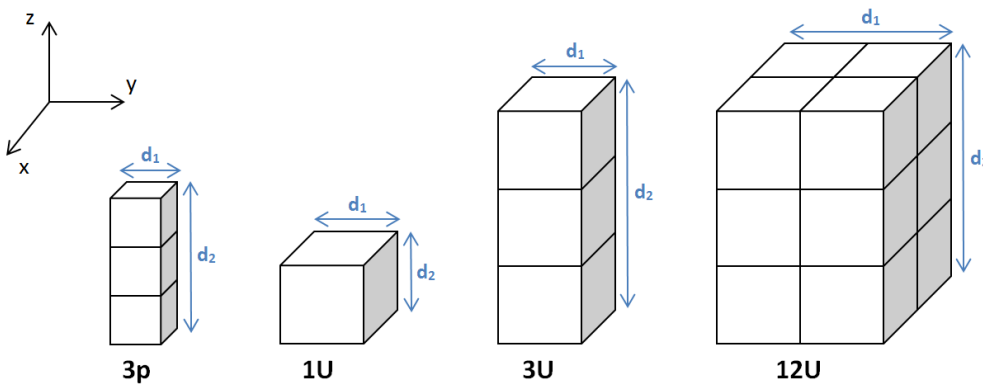


Figure 30: Simplified geometries of the small satellite formats considered in the study.

Table 3: Spacecraft data used for the analysis.

	Symbol	Unit	1p	1U	3U	12U
Spacecraft dimensions	d_1	[cm]	5	10	10	20
	d_2	[cm]	15	10	30	30
Initial mass (wet)	M_0	[kg]	0.5	1	3.6	24
Principal moments of inertia	I_z	[kg·m ²]	$2.1 \cdot 10^{-4}$	$1.7 \cdot 10^{-3}$	$6 \cdot 10^{-3}$	$1.6 \cdot 10^{-1}$
	I_x	[kg·m ²]	$10.5 \cdot 10^{-4}$	$1.7 \cdot 10^{-3}$	$3 \cdot 10^{-2}$	$2.6 \cdot 10^{-1}$
	I_y	[kg·m ²]	$10.5 \cdot 10^{-4}$	$1.7 \cdot 10^{-3}$	$3 \cdot 10^{-2}$	$2.6 \cdot 10^{-1}$
Average satellite power	P_{sat}	[W]	2	4	12	25

For what concerns the applications, four different cases have been considered and will be discussed more in detail in the following sections:

- **Case 1: attitude control of an Earth-pointing satellite in LEO** (Low Earth Orbit). In this case the thrusters are used (in pairs) to maintain the spacecraft attitude, allowing for imaging or any other applications that require accurate pointing. Although attitude control, especially in LEO, can also be done using different actuators (magnetic torquers, reaction wheels), the results related to this case give a good insight on what kind of micro-propulsion would be appropriate to cover applications requiring precise thrust level and accurate pointing.
- **Case 2: drag compensation for altitude maintenance in LEO**. In this case one single thruster is used to compensate the drag forces generated by the relatively high air density in LEO, in order for the spacecraft to be maintained within a given range of altitudes. This case can also be more generically related to formation flying maneuvers in LEO, where the main cause for bringing the satellites out of the formation is the drag force.
- **Case 3: station keeping in GEO** (Geostationary Earth Orbit). Although small satellites are not typically used in GEO, this case offers very similar requirements to formation flying maneuvers in high-altitude orbits, where atmospheric drag does not play a significant role anymore and the main sources of deviations from the nominal spacecraft trajectory are secular orbital disturbances.
- **Case 4: interplanetary transfer**, with two specific sub-cases considered: Lunar transfer (from Low Lunar Orbit to a halo orbit around the Earth-Moon Lagrangian point L2), and Mars transfer (from Mars Transfer Orbit to Low Mars Orbit). The Lunar transfer case is representative of several recently proposed small satellite missions around the Moon, while the Mars transfer case resembles a situation where the spacecraft is brought to Mars Transfer Orbit by an external kick stage and has to transfer autonomously from there to Mars, using its own micro-propulsion system.

3.2 Attitude control of an Earth-pointing satellite in LEO

The spacecraft is assumed to be constantly pointing towards ground with its z-axis (see Figure 30) for imaging, antenna pointing or other Earth observation purposes. The z-axis in the body-fixed system of the satellite is therefore assumed parallel to the Nadir direction, with a maximum acceptable deviation of 1 deg. The range of altitudes considered in this case is from **300 km** (minimum) to **700 km** (maximum). It is assumed that a pair of thrusters are installed in such a way to generate opposite thrust forces of same magnitude, perpendicularly to the x-axis (or the y-axis, depending on the direction along which the disturbance torque acts), at a distance from each other equal to d_2 (see Figure 30), which is the maximum possible moment arm allowed by the geometry of the spacecraft in order to produce torque only around the x-axis and not around the other axes. The thrusters are assumed to be operated continuously in

order to counteract the disturbance torques acting on the spacecraft. The study is conducted for a minimum operational lifetime in orbit of **1 year**, and a maximum one of **5 years**.

Under these assumptions, two periodic disturbance torques are typically dominant on the spacecraft: the gravity gradient and the magnetic field disturbance. Simplified equations to estimate the worst-case value of these disturbance torques can be obtained from Larson and Wertz [11]. The gravity gradient disturbance torque T_g can be calculated using:

$$T_g = \frac{3\mu}{2R^3} \cdot |I_z - I_y| \cdot \sin(2\theta_{\max}) \quad (3.1)$$

where μ is the Earth's gravity constant, R is the orbit radius and θ_{\max} is the maximum acceptable angular deviation of the z-axis from its nominal direction parallel to Nadir.

The worst-case magnetic field disturbance torque T_m is given by:

$$T_m = \frac{2M_E}{R^3} \cdot D_M \quad (3.2)$$

where M_E is the Earth's magnetic moment, and D_M is the residual magnetic dipole of the spacecraft. The value of D_M is not easy to calculate and depends on the specific characteristics of the hardware installed in the satellite; the values used for this study are **0.002 Am²** for the 3p format (typical worst-case value currently used in the design of the Delfi-PQ satellite) and **0.2 Am²** for all other formats (typical value found in literature for CubeSats).

From equations (3.1) and (3.2), with the numbers used in this study, it is very clear that in all the cases considered here $T_g \ll T_m$. Therefore, all the results presented in the following will be referred to T_m only, neglecting the contributions of the gravity gradient disturbance torque. The minimum acceptable thrust to counteract the disturbance torque can be calculated with:

$$F_T \cdot d_2 = T_m \rightarrow F_T = \frac{T_m}{d_2} \quad (3.3)$$

The Delta-V change required by the propulsion system during the whole spacecraft lifetime can then be calculated recalling that the total impulse produced by the two thrusters is equal to the linear momentum change that would be produced in case they were used to accelerate the spacecraft:

$$2F_T \cdot t_b = M_0 \cdot \Delta v \rightarrow \Delta v = \frac{2F_T \cdot t_b}{M_0} \quad (3.4)$$

where t_b is the burn time of each of the two thrusters; in this particular application, where continuous thrust is considered, it coincides with the spacecraft operational lifetime in orbit. The required propellant mass can then be calculated as a function of the specific impulse using equations (1.2) and (1.3):

$$\Delta v = g_0 I_{sp} \cdot \ln\left(\frac{M_0}{M_0 - M_p}\right) \rightarrow M_p = M_0 \left[1 - e^{-\frac{\Delta v}{g_0 I_{sp}}} \right] \quad (3.5)$$

Finally, from historical data of satellites used for similar applications, it can be assumed that the total wet mass of the propulsion system (dry mass plus propellant mass) shall be no more than **30%** of the initial spacecraft mass M_0 . This allows to derive an expression for the maximum acceptable dry mass M_{dry} of the propulsion system:

$$M_{dry} + M_p \leq 0.3M_0 \rightarrow M_{dry} \leq M_0 \left[e^{-\frac{\Delta v}{g_0 I_{sp}}} - 0.7 \right] \quad (3.6)$$

Equation (3.6) is plotted in Figures 31 and 32 for the minimum and maximum orbit altitude and all the small satellite formats considered. The two Figures refer, respectively, to the minimum and maximum assumed operational lifetime.

Additionally, given the assumption of continuous thrusting and again from historical data of satellites used for similar applications, it is assumed that the propulsion system can use no more than **40%** of the average satellite power, in order for enough power to be left to the other sub-systems. In Figure 33, the thrust and power limits for this particular application are shown for all the satellite formats considered.

The first noticeable aspect in the results is that the altitude does not influence the micro-propulsion choice significantly and (at least for the range of altitudes considered in this study) the selection can be made independently on the altitude.

The most challenging satellite format is the **1U**, for which basically none of the current state-of-the-art systems meets the dry mass requirements.

For the **3p** format, some electric propulsion concepts meet the dry mass requirements (electrospray, ion thrusters, Pulsed Plasma Thrusters), but none of them meets the stringent power requirements offered by this format, at least in the current state-of-the-art scenario.

For the **3U** format, a few electric propulsion concepts meet the power and thrust requirements (electrospray, Pulsed Plasma Thrusters, resistojet, vacuum arc). However, among these, only electrospray, Pulsed Plasma Thrusters and vacuum arc also meet the dry mass requirements for the 1-year orbital lifetime case, while only one vacuum arc option and (marginally) one electrospray option meet them for the 5-years orbital lifetime case. The preferred solution for 1-year orbital lifetime seems to be the Pulsed Plasma Thrusters, given the larger number of currently available alternatives that meet all requirements.

Finally, for the **12U** format, all micro-propulsion systems meet the requirements for the 1-year orbital lifetime case, and most of them (with the only exception of cold gas and resistojet) are suitable for the 5-years case too. However, analysis of the thrust-power limits shows that only some electric propulsion options are suitable (electrospray, Pulsed Plasma Thrusters, resistojets, Radio-Frequency thrusters, vacuum arc). The optimal solutions for the 1-year case, for variety and performance range, are cold gas and Pulsed Plasma Thrusters. For the 5-years case, preference would be given to electrospray and Pulsed Plasma Thrusters.

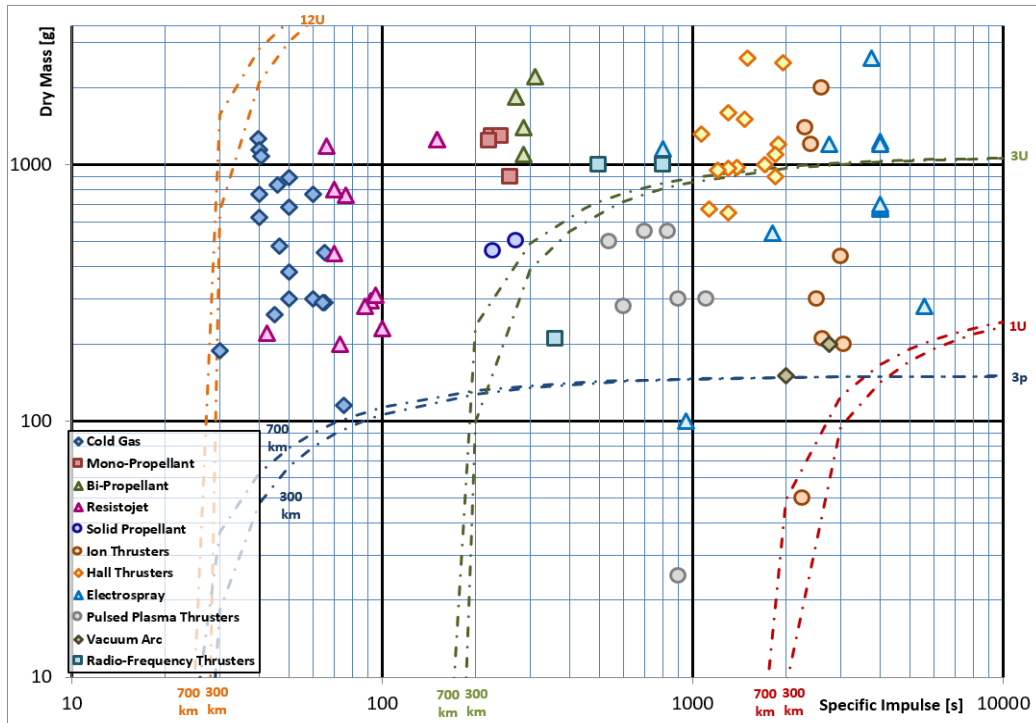


Figure 31: Maximum acceptable dry mass as a function of the specific impulse, for all considered satellite formats and a lifetime of 1 year (case 1: attitude control in LEO).

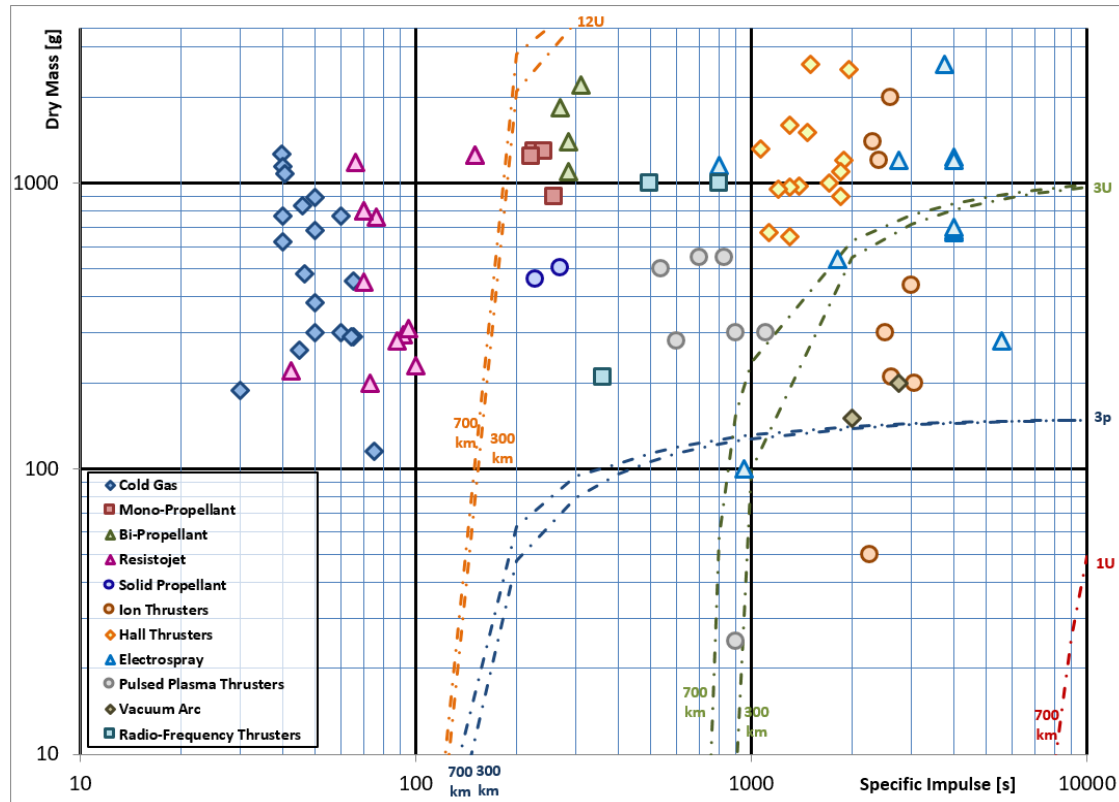


Figure 32: Maximum acceptable dry mass as a function of the specific impulse, for all considered satellite formats and a lifetime of 5 years (case 1: attitude control in LEO).

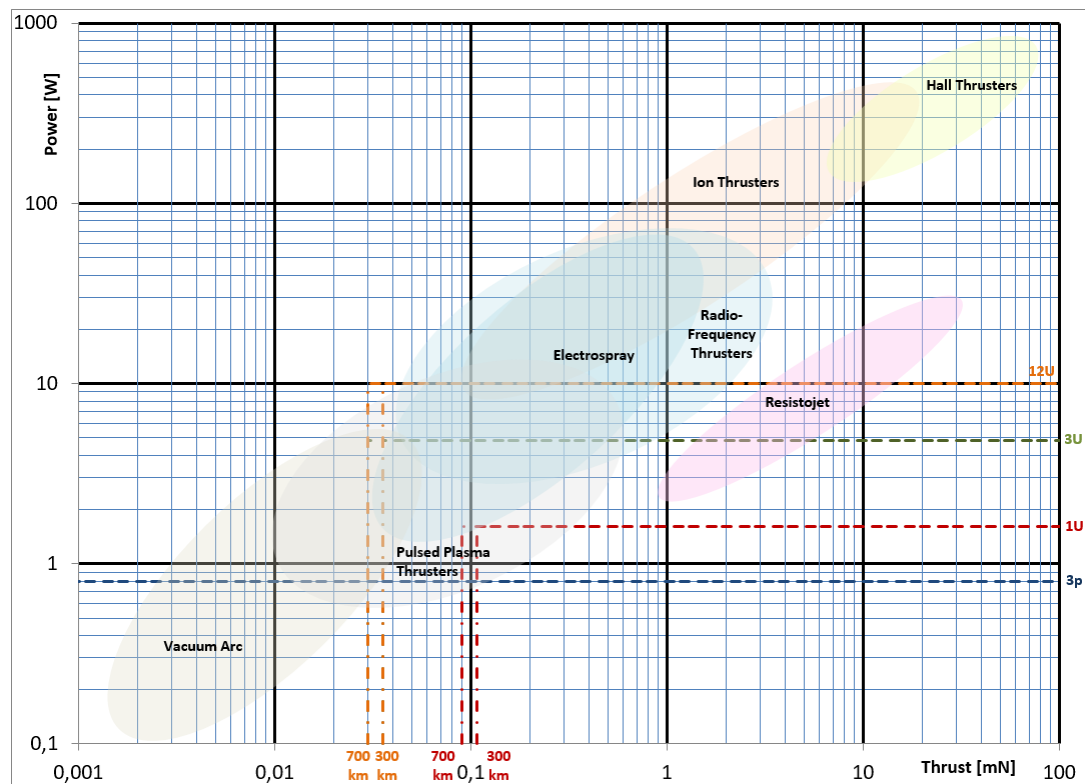


Figure 33: Micro-propulsion thrust and power limits, for all considered satellite formats (case 1: attitude control in LEO).

3.3 Drag compensation for altitude maintenance in LEO

The spacecraft is assumed to fly with orbital velocity constantly parallel to its z-axis (see Figure 30). The range of altitudes considered for this application is from **150 km** (minimum, with spacecraft operational lifetime in the range **1-3 months**) to **300 km** (maximum, with spacecraft operational lifetime in the range **1-5 years**). It is assumed that the atmospheric drag is compensated by one single thruster, firing in a direction exactly parallel to the spacecraft z-axis. The correction manoeuvre is performed when the altitude falls outside its nominal value by a given amount, that ranges from **1 km** (most accurate) to **20 km** (least accurate).

Also in this case, simplified equations to estimate the orbital decay caused by atmospheric drag can be obtained from Larson and Wertz [11]. The variations of orbit radius and orbital velocity per orbit, ΔR_{rev} and ΔV_{rev} , can be calculated as:

$$\Delta R_{rev} = -2\pi \left(\frac{C_d A}{M_0} \right) \rho R^2 \quad (3.7)$$

$$\Delta V_{rev} = \pi \left(\frac{C_d A}{M_0} \right) \rho R V \quad (3.8)$$

where ρ is the atmospheric density at the given altitude, V is the orbital velocity, C_d is the spacecraft drag coefficient, A is the spacecraft frontal area perpendicular to the flight direction. For the given parallelepiped spacecraft shape, a C_d equal to **2.2** can be assumed, while the frontal area, under the given assumptions, will be equal to d_l^2 (see Figure 30).

The atmospheric density varies not only with altitude, but is also subject to periodic variations due to the solar cycles. For this study, however, it will be considered constant and equal to its average value during a solar cycle period, which according to [11] is equal to **$1.81 \cdot 10^{-9} \text{ kg/m}^3$** (at 150 km altitude), or **$1.95 \cdot 10^{-11} \text{ kg/m}^3$** (at 300 km altitude).

Finally, the orbital velocity V and orbital period T can be calculated using the following equations:

$$V = \sqrt{\frac{\mu}{R}} \quad (3.9)$$

$$T = 2\pi \sqrt{\frac{R^3}{\mu}} \quad (3.10)$$

It is now possible to estimate the total Delta-V change required to the propulsion system, by recalling that the total number of orbits during the spacecraft lifetime t_{life} is equal to t_{life} divided by the orbital period T :

$$\Delta v = \Delta V_{rev} \cdot \frac{t_{life}}{T} \quad (3.11)$$

Also in this case, analogously to the previous application described in section 3.2, it can be assumed that the total wet mass of the propulsion system (dry mass plus propellant mass) shall be no more than **30%** of the initial spacecraft mass M_0 . This allows to use equation (3.6) again for the maximum acceptable dry mass M_{dry} of the propulsion system as a function of the specific impulse. The result is plotted in Figures 34 and 35 for the minimum and maximum spacecraft lifetime and all the small satellite formats considered. The two Figures refer, respectively, to the minimum and maximum assumed altitudes (150 km and 300 km).

The number of orbits after which it is necessary to perform an altitude correction manoeuvre is given by the required altitude variation per manoeuvre ΔR_{man} (ranging from 1 km to 20 km

in the current study), divided by the altitude variation per orbit ΔR_{rev} . The Delta-V value required by each altitude correction manoeuvre can then be calculated as:

$$\Delta V_{man} = \frac{\Delta R_{man}}{\Delta R_{rev}} \cdot \Delta V_{rev} \quad (3.12)$$

In this study, it is assumed that the power P usable by the propulsion system for each altitude correction manoeuvre is such that the **full amount of energy** produced by the satellite during its full previous orbit is used by the propulsion system to perform the manoeuvre. This allows to calculate the burn time t_b in the following way:

$$P_{sat} \cdot T = P \cdot t_b \rightarrow t_b = \frac{P_{sat}}{P} \cdot T \quad (3.13)$$

Note, however, that equation (3.13) is not applicable to cases when multiple manoeuvres per orbit are needed, as it typically happens at low altitude (150 km) and high control accuracy (1 km). In these cases, it is assumed instead that, similarly to the previous study case related to continuous thrusting for attitude control purposes, **40%** of the energy produced by the satellite during the whole period between two successive maneuvers is used. Equation (3.13) can then be rewritten as:

$$0.4P_{sat} \cdot \frac{\Delta R_{man}}{\Delta R_{rev}} \cdot T = P \cdot t_b \rightarrow t_b = \frac{0.4P_{sat}}{P} \cdot \frac{\Delta R_{man}}{\Delta R_{rev}} \cdot T \quad (3.14)$$

Finally, an equation similar to (3.4) can be used to estimate the power required by the propulsion system as a function of the thrust level used to accelerate the spacecraft:

$$M_0 \cdot \Delta V_{man} = F_T \cdot t_b \rightarrow P = \begin{cases} \frac{P_{sat} \cdot T}{M_0 \cdot \Delta V_{man}} \cdot F_T, & \text{for } \frac{\Delta R_{man}}{\Delta R_{rev}} > 1 \\ \frac{0.4P_{sat} \cdot T}{M_0 \cdot \Delta V_{man}} \cdot \frac{\Delta R_{man}}{\Delta R_{rev}} \cdot F_T, & \text{for } \frac{\Delta R_{man}}{\Delta R_{rev}} < 1 \end{cases} \quad (3.15)$$

Equation (3.15) is plotted in Figure 36, for all satellite formats and study cases considered. Note that for all the satellite formats considered, the lines related to low control accuracy (20 km) are very close to each other independently on the altitude (150 km or 300 km). For the high control accuracy case (1 km), the power curve is significantly lower in the case of lower altitude (150 km), due to the fact that in this case multiple correction maneuvers per orbit would be needed and therefore less power is available per maneuver.

The first consideration that can be made very clearly from analysis of Figure 36 is that the case of low control accuracy (20 km) is very difficult to be performed by electric propulsion systems, given the higher Delta-V per manoeuvre required which, in turn, means longer burn duration and lower available power per burn. No electric propulsion solutions are available for the 12U format and the only available one for the other formats, the resistojet, does not meet the given dry mass and specific impulse requirements (Figures 34 and 35), except for the very specific case of 3U format at higher altitude (300 km) and shorter operational lifetime (1 year). This shows that, in terms of power and thrust requirements, it is always preferable to go for high control accuracy (1 km). All the considerations in the following will therefore be referred to this specific case.

For both **3p** and **1U** formats, none of the available micro-propulsion options meets at the same time the thrust, power, dry mass and specific impulse requirements for the lower altitude case (150 km). However, for the higher altitude case (300 km), a few electrospray options meet all the given requirements, even at the maximum spacecraft operational lifetime of 5 years.

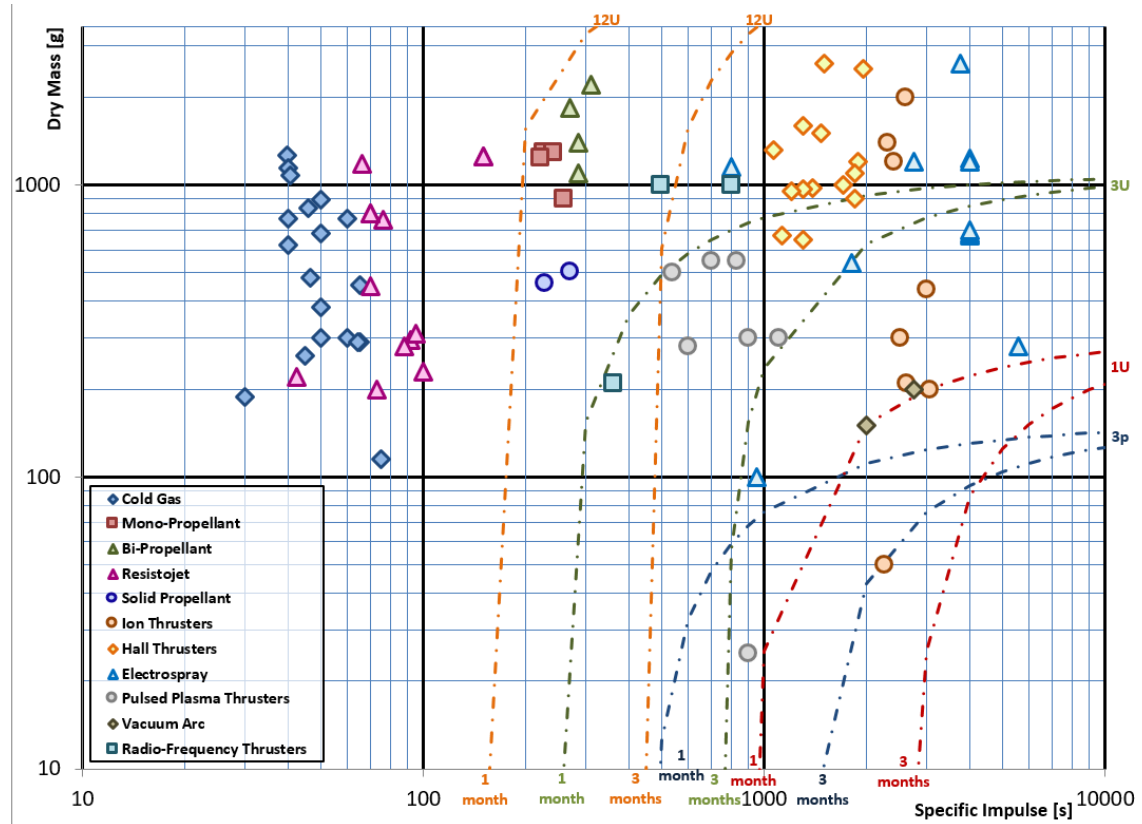


Figure 34: Maximum acceptable dry mass as a function of the specific impulse, for all considered satellite formats and 150 km altitude (case 2: altitude maintenance in LEO).

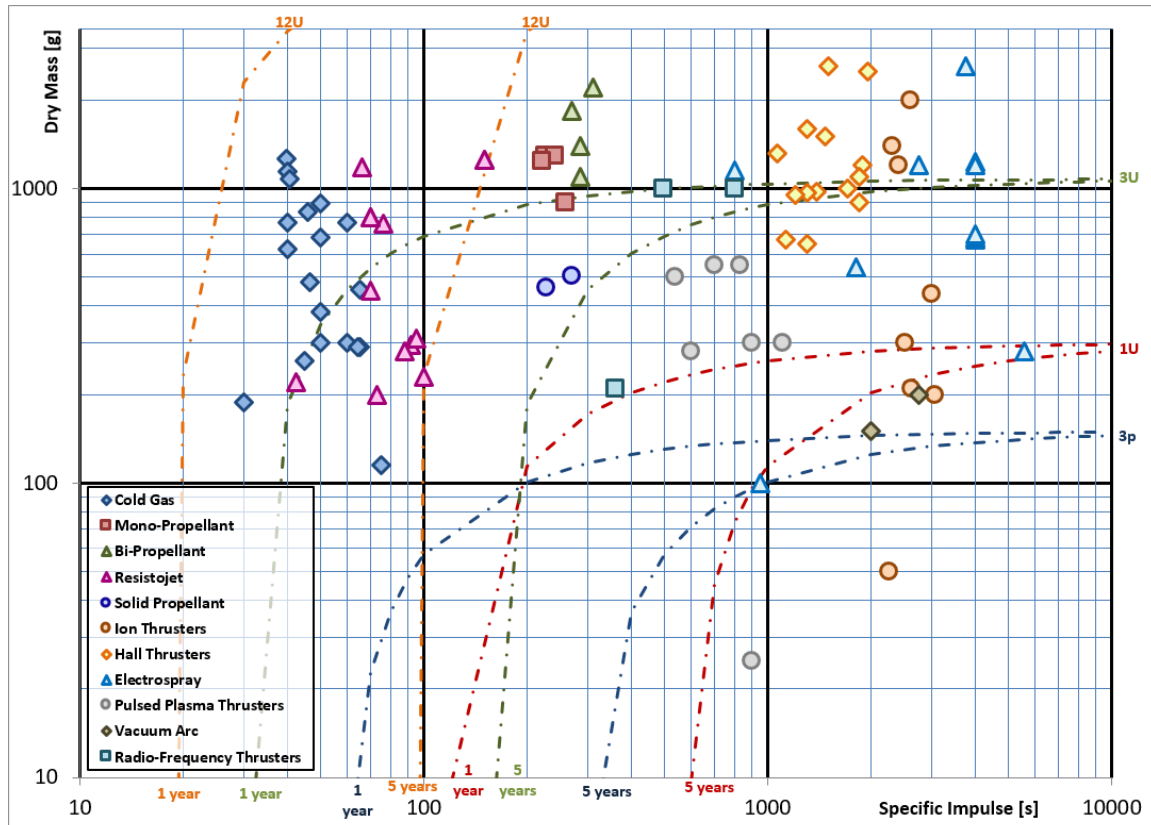


Figure 35: Maximum acceptable dry mass as a function of the specific impulse, for all considered satellite formats and 300 km altitude (case 2: altitude maintenance in LEO).

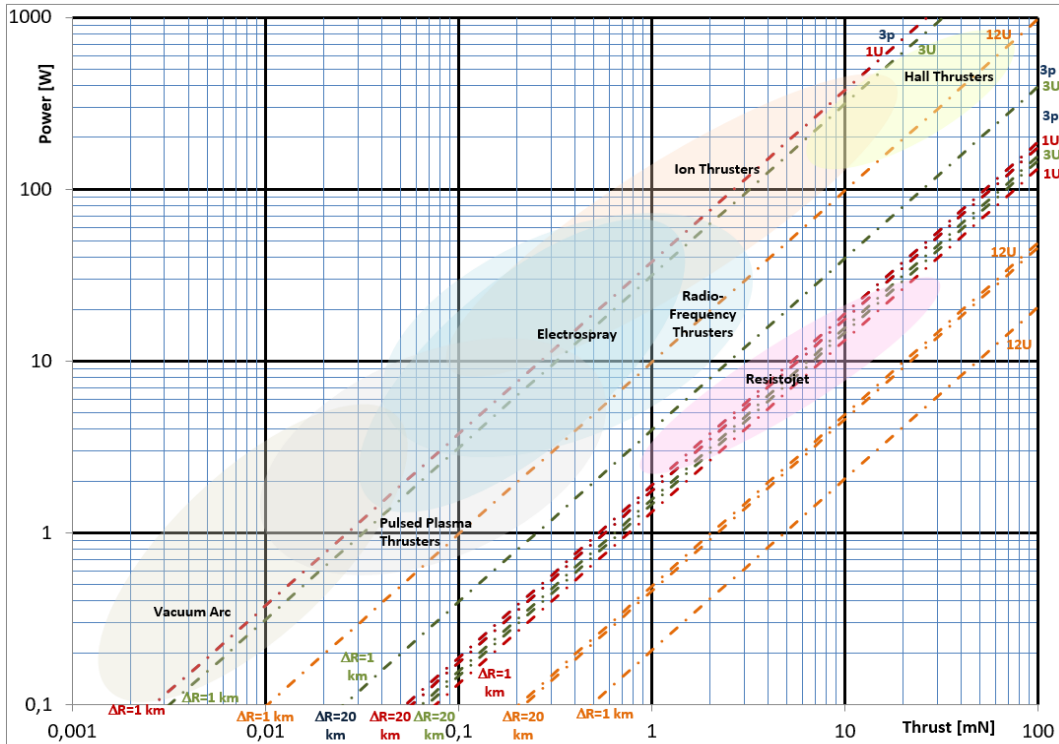


Figure 36: Maximum acceptable micro-propulsion power as a function of thrust, for all considered satellite formats (case 2: altitude maintenance in LEO).

Also for the **3U** format, none of the available micro-propulsion options meets the given requirements in the low altitude case (150 km). In the high altitude case (300 km), several alternatives allow to meet the maximum lifetime requirement of 5 years (electrospray, ion, Pulsed Plasma Thrusters, Hall effect thrusters, Radio-Frequency thrusters). Among these, electrospray and Pulsed Plasma Thrusters are preferable, given the variety and performance range of options available. Reduced lifetime, but still longer than the given minimum requirement of 1 year, can be obtained with solid propellant thrusters, cold gas and resistojets.

Finally, for the **12U** format, the low altitude requirements are met, only for the shorter lifetime case (1 month), by solid propellant thrusters, mono-propellants or bi-propellants. At high altitude, the longer lifetime requirement of 5 years is met by a wide range of micro-propulsion types and options (Hall effect thrusters, Radio-Frequency thrusters, Pulsed Plasma Thrusters, solid propellant thrusters, mono-propellants, bi-propellants). A shorter lifetime, but still longer than the given minimum of 1 year, can be obtained with cold gas or resistojets. In both cases (low altitude and high altitude), mono-propellants are considered the preferred option, given their less stringent requirements in terms of power.

3.4 Station keeping in GEO

The spacecraft is assumed to fly in a GEO orbit, with station keeping manoeuvres (both North-South and East-West) performed by one single thruster firing in the required direction. The study is conducted for a minimum operational lifetime in GEO orbit of **1 year**, and a maximum one of **5 years**.

The Delta-V for station keeping in GEO orbit can be obtained from Larson and Wertz [11], and is typically equal to **51.4** m/s per year (for North-South station keeping) and **1.715** m/s per year (for East-West station keeping). Also in this case, it is assumed that the total wet mass of the propulsion system (dry mass plus propellant mass) shall be no more than **30%** of the initial spacecraft mass M_0 . This allows to use again equation (3.6) for the maximum acceptable dry mass M_{dry} of the propulsion system as a function of the specific impulse, with Delta-V given by the sum of the Delta-V requirements for North-South and East-West station

keeping. The result is plotted in Figure 37 for the minimum and maximum spacecraft lifetime and all the small satellite formats considered.

The thrust requirements for this application are derived by setting a value for the allowed angular drift from the nominal position in GEO. Two values are considered for this drift: **0.1 degrees** (higher station keeping accuracy) and **1 degree** (lower station keeping accuracy). Furthermore, it is assumed that the propulsion system minimum burn time per manoeuvre ranges between **1 s** (short burn) and **10 s** (long burn).

From [11], it can be found that the typical drift in GEO in the East-West direction is **73 degrees per year**, while the typical drift in GEO in the North-South direction is **15 degrees in 55 years**. These drifts, divided by the maximum allowed drift for the spacecraft (0.1 or 1 degrees), allow to calculate the number of manoeuvres per year that need to be performed and, therefore, the required Delta-V per manoeuvre ΔV_{man} . The usual equation for the total impulse as a function of linear momentum variation can then be used to estimate the maximum thrust requirement:

$$F_T \cdot t_b = M_0 \cdot \Delta V_{man} \rightarrow F_T = \frac{M_0 \cdot \Delta V_{man}}{t_b} \quad (3.16)$$

Using the numbers provided above, it can be easily seen that the East-West drift requirement is always significantly stricter than the North-South one in terms of thrust. All the results presented in the following will therefore be related to the East-West case.

Finally, given the non-continuous thrusting assumption and the relatively infrequent manoeuvres required, it is assumed that a large amount of the available power can be used by the micro-propulsion system during the manoeuvre, up to **80%** of the average satellite power. In Figure 38, the thrust and power limits for this particular application are shown for all the satellite formats and operational conditions (allowed angular drift, burn time per manoeuvre) considered in the study.

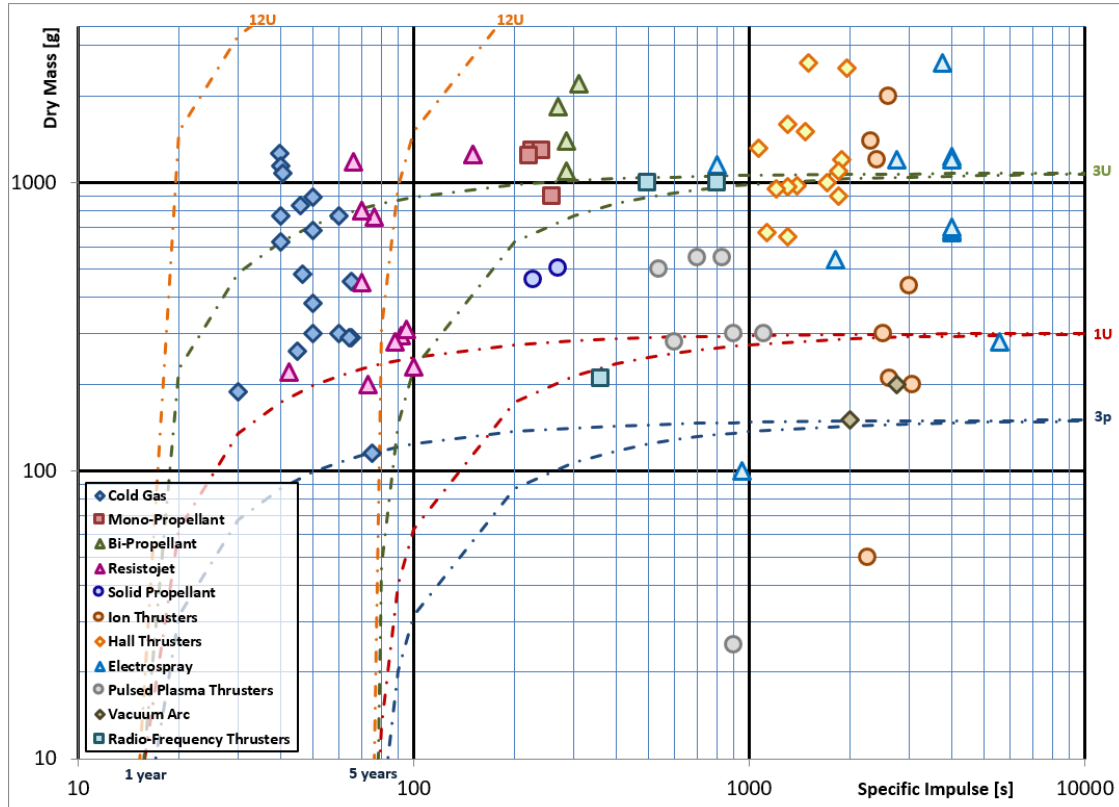


Figure 37: Maximum acceptable dry mass as a function of the specific impulse, for all considered satellite formats (case 3: station keeping in GEO).

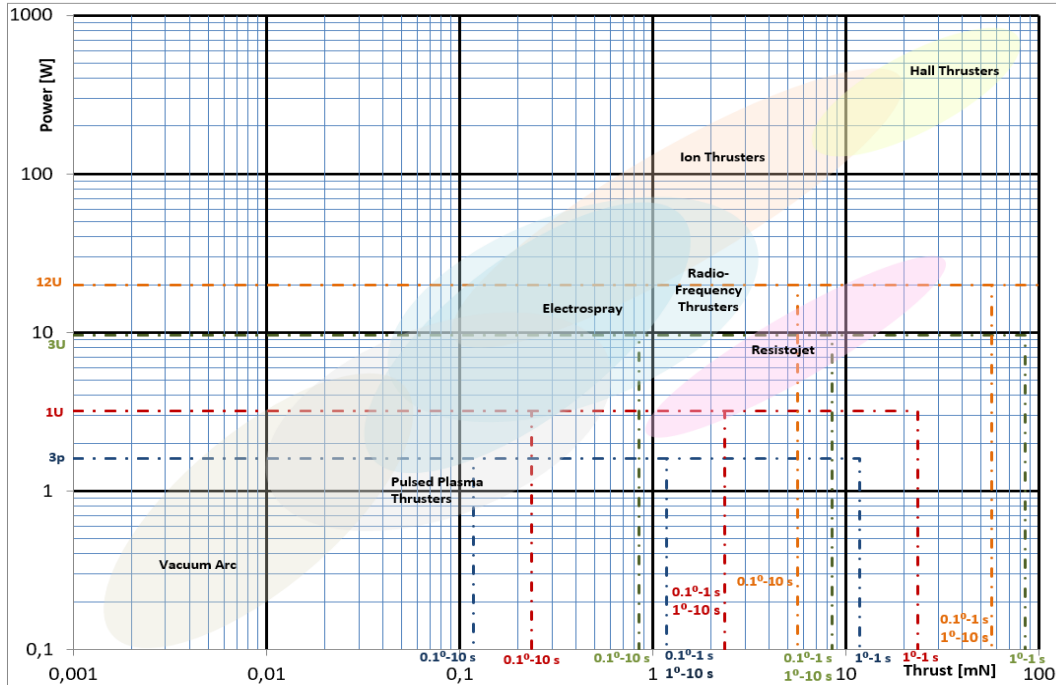


Figure 38: Maximum acceptable micro-propulsion power as a function of the maximum thrust, for all considered satellite formats (case 3: station keeping in GEO).

For the **3p** format, only one electrospray option, among the state-of-the-art available ones, allow to meet all the given combinations of requirements for this application. The same option is also applicable to the **1U** format, for which the requirements are however met also by one vacuum arc option, preferred in this case given the better margin it offers with respect to the required performance; for this format, there is also one single cold gas option that allows to meet the short lifetime requirement of 1 year (but not the longer one of 5 years).

A better choice is offered by the **3U** format, where several alternatives allow to meet the maximum lifetime requirement of 5 years (electrospray, Pulsed Plasma Thrusters, Radio-Frequency thrusters, vacuum arc thrusters, solid propellant thrusters). Among these, electrospray and Pulsed Plasma Thrusters are preferable, given the variety and performance range of options available. Reduced lifetime, but still longer than the given minimum requirement of 1 year, can be obtained with cold gas, resistojets and mono-propellant.

Finally, for the **12U** format, the longer lifetime requirement of 5 years is met by a wide range of micro-propulsion types and options (Radio-Frequency thrusters, Pulsed Plasma Thrusters, electrospray, vacuum arc thrusters, ion thrusters, solid propellant thrusters, mono-propellants, bi-propellants, resistojets). In this case, mono-propellants are considered the preferred option, given their less stringent requirements in terms of power. A shorter lifetime, but still longer than the given minimum of 1 year, can be obtained with cold gas thrusters.

3.5 Interplanetary transfer – Low Lunar Orbit to halo orbit

For this case, from literature and historical data, a total Delta-V of **150 m/s** is assumed in case the transfer is operated in high-thrust mode, which typically means a thrust duration of less than **60 min** in order to reduce the gravity loss effects on the Delta-V to less than 10%. When the available thrust does not allow for this thrust duration, the transfer is performed in low-thrust mode, with an assumed Delta-V requirement doubled to **300 m/s**.

In the high-thrust case, since the thrust time is shorter, it is assumed that a large amount of the available power can be used by the micro-propulsion system during the manoeuvre, up to **80%** of the average satellite power. For the low-thrust case, given the longer thrust duration, the usual limitation of no more than **40%** of the average satellite power is applied to the micro-propulsion system. The power and thrust requirements posed by this application are

plotted, for all the small satellite formats considered, in Figure 39. It shall be noted, however, that the Figure refers only to electric propulsion options. For the other micro-propulsion types, the following considerations apply after calculating the high-thrust threshold and comparing it to the thrust data shown in Chapter 2:

- **3p, 1U** formats: cold gas, solid, monopropellant and bi-propellant thrusters are all high-thrust options.
- **3U** format: cold gas are a low-thrust option; solid, monopropellant and bi-propellant thrusters are high-thrust.
- **12U** format: cold gas, monopropellant and bi-propellant thrusters are low-thrust options; solid propellant thrusters are high-thrust.

From historical data of satellites used for similar applications, it can be assumed that the total wet mass of the propulsion system (dry mass plus propellant mass) is significantly higher than the other applications considered in this study, and therefore shall be no more than **50%** of the initial spacecraft mass M_0 . In this case, equation (3.6) for the maximum dry mass becomes:

$$M_{dry} + M_P \leq 0.5M_0 \rightarrow M_{dry} \leq M_0 \left[e^{-\frac{\Delta v}{g_0 I_{sp}}} - 0.5 \right] \quad (3.17)$$

Equation (3.17) is plotted in Figure 40 for the minimum and maximum orbit altitude and all the small satellite formats considered, for both high-thrust and low-thrust cases.

For the **3p** format, only one vacuum arc option (low-thrust case) meets the given power, dry mass and specific impulse requirements.

For the **1U** format, one vacuum arc and one electrospray option, among the state-of-the-art available ones, allow to meet all the given combinations of requirements under the low-thrust assumption, as well as several Pulsed Plasma Thruster options, which are preferred in this case given the wider range of concepts and performance characteristics available. Only one cold gas option meets the given requirements for the high-thrust case.

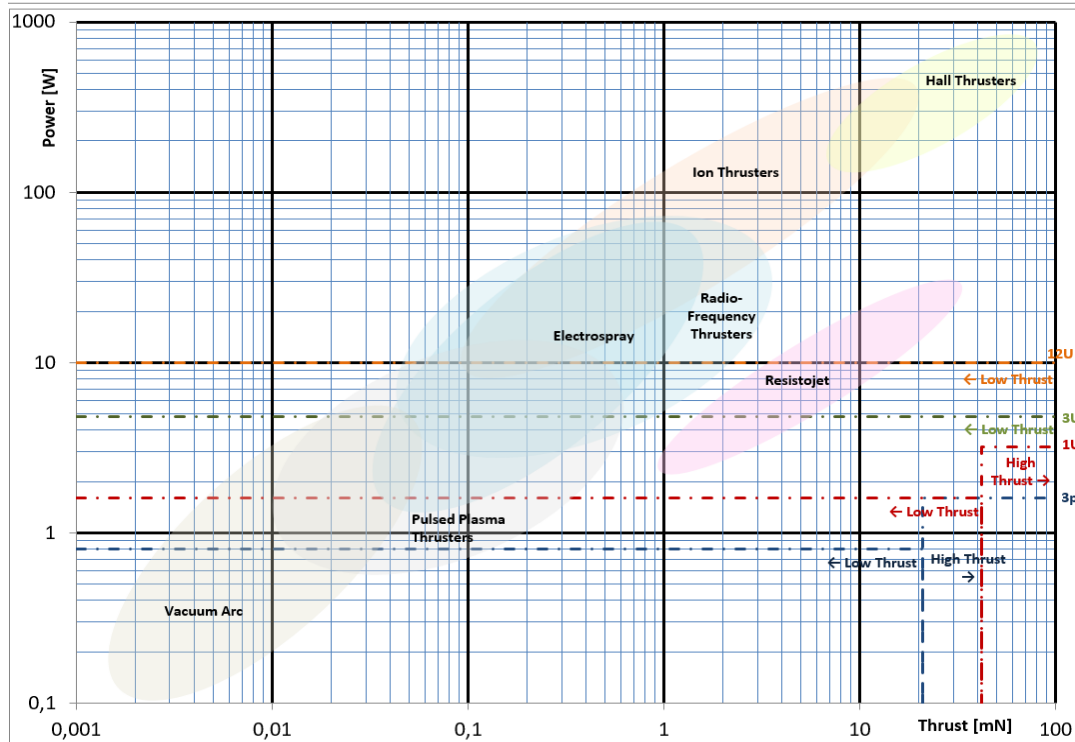


Figure 39: Maximum acceptable micro-propulsion power as a function of thrust, for all considered satellite formats (case 4a: Lunar transfer).

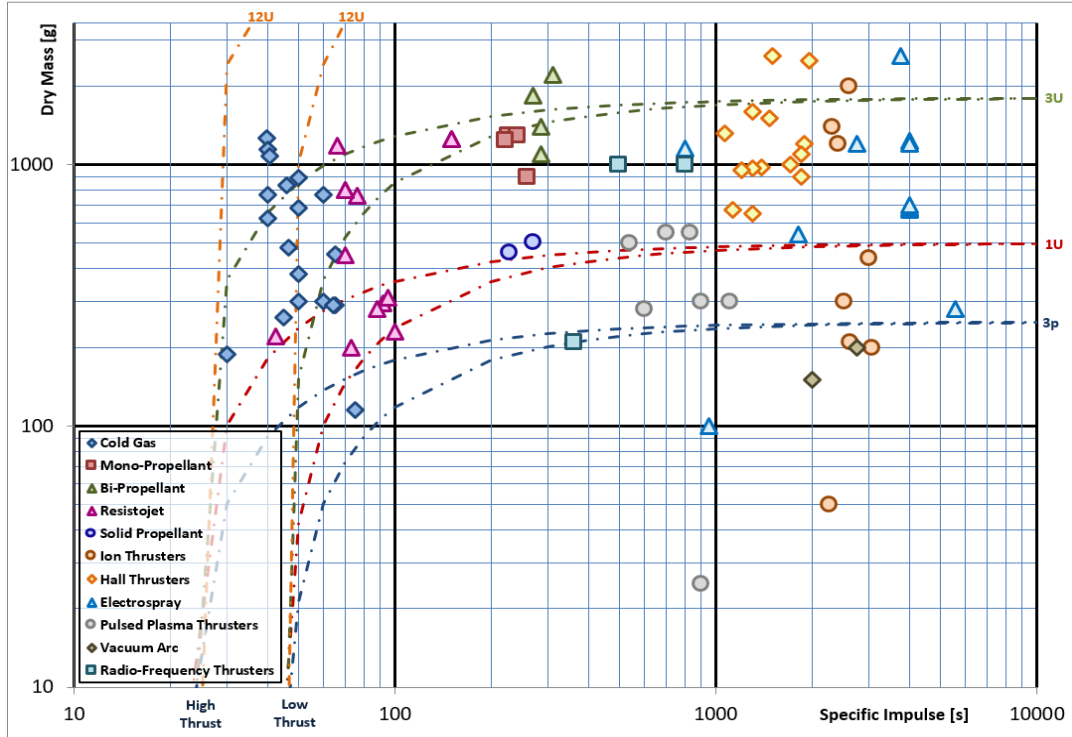


Figure 40: Maximum acceptable dry mass as a function of the specific impulse, for all considered satellite formats (case 4a: Lunar transfer).

For the **3U** format, a wide range of options are available under the low-thrust assumption: cold gas, resistojet, Pulsed Plasma Thrusters, vacuum arc, electrospray, Radio-Frequency thrusters. The preferred options in this case are the cold gas one (for its simplicity and lower power requirements) and the Pulsed Plasma Thrusters (for the wide margin they offer with respect to the requirements). Some solutions are available too for the high-thrust case: solid propellant, bi-propellant and mono-propellant thrusters. The preferred options in this case are solid propellant (given their lower dry mass) and mono-propellant thrusters (given their simplicity and better controllability). A similar situation applies to the **12U** format, with the only difference that bi-propellant and mono-propellant thrusters fall in this case under the low-thrust options instead of the high-thrust ones.

3.6 Interplanetary transfer – Mars Transfer Orbit to Low Mars Orbit

The same considerations and requirements as in the Lunar transfer case apply to the Mars transfer too, with however significantly more challenging Delta-V requirements: the total Delta-V to be provided by the micro-propulsion system is assumed equal to **2500 m/s** in high-thrust mode, and **5000 m/s** in low-thrust mode. The results are shown in Figures 41 and 42.

Similarly to the Moon transfer case, it shall be noted that Figure 41 refers only to electric propulsion options. For the other micro-propulsion types, the following considerations apply after calculating the high-thrust threshold and comparing it to the thrust data shown in Chapter 2:

- **3p** format: cold gas are a low-thrust option; solid, monopropellant and bi-propellant thrusters are high-thrust.
- **1U, 3U, 12U** formats: cold gas, monopropellant and bi-propellant thrusters are low-thrust options; solid propellant thrusters are high-thrust.

For the **3p** format, none of the available micro-propulsion options meets the given power, dry mass and specific impulse requirements, for both the low-thrust and high-thrust cases.

For the **1U** format, one vacuum arc and one electrospray option, among the state-of-the-art available ones, allow to meet all the given combinations of requirements under the low-thrust

assumption. The preferred option in this case is the vacuum arc one, given the wider performance margin it offers with respect to the requirements. No options are available for the high-thrust case.

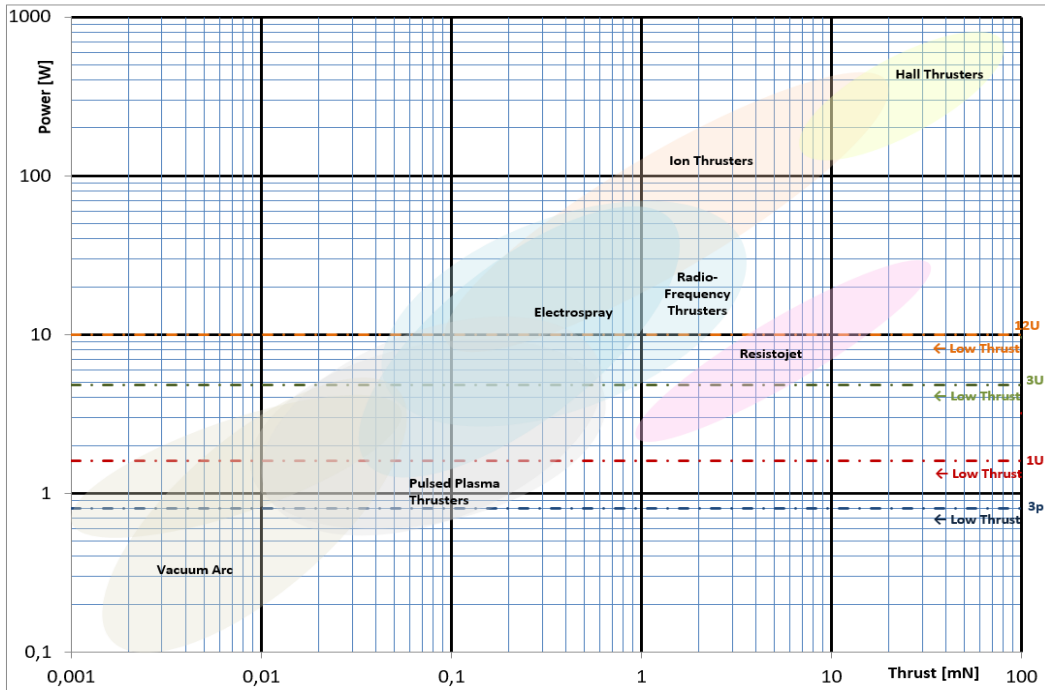


Figure 41: Maximum acceptable micro-propulsion power as a function of thrust, for all considered satellite formats (case 4b: Mars transfer).

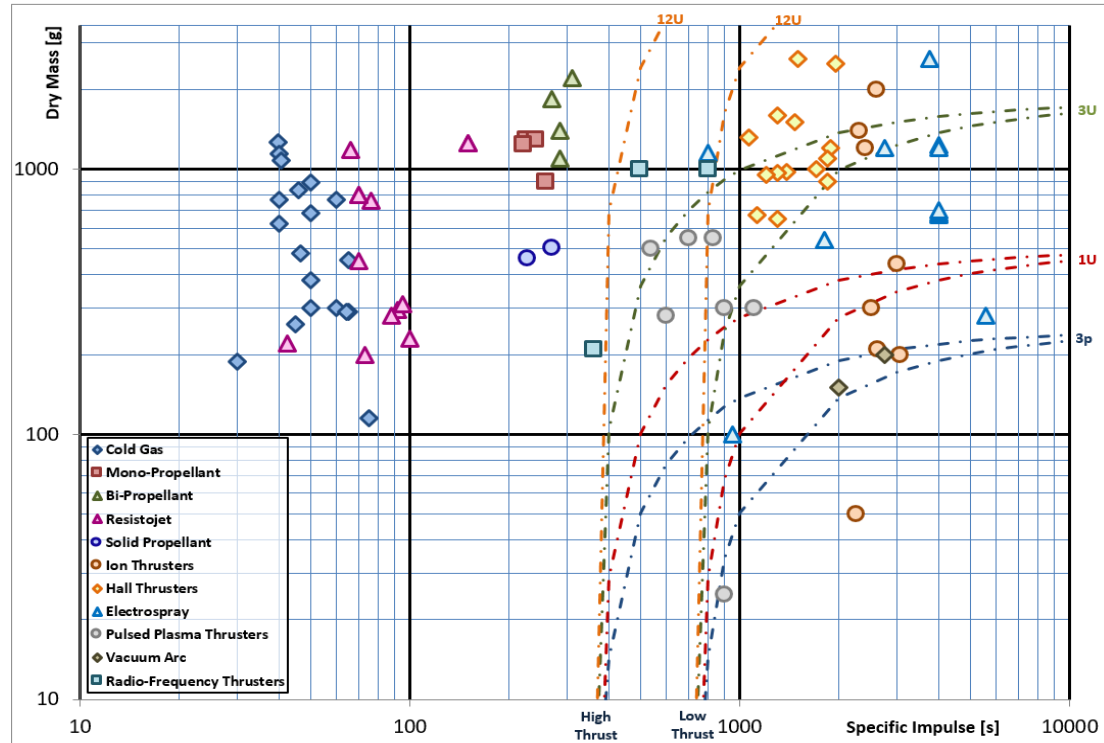


Figure 42: Maximum acceptable dry mass as a function of the specific impulse, for all considered satellite formats (case 4b: Mars transfer).

For the **3U** format, one vacuum arc and one Pulsed Plasma Thruster option, among the state-of-the-art available ones, allow to meet all the given combinations of requirements under the

low-thrust assumption, as well as several electrospray options, which are preferred in this case given the wider range of concepts and performance characteristics available. No options are available for the high-thrust case. A similar result can be found for the 12U format.

3.7 Summary and conclusions

Tables 4, 5, 6 and 7 summarize the results of the analysis conducted in this chapter, indicating for each application and each small satellite format what are the applicable and partially applicable options and, among the applicable ones, the preferred solution(s) according to the considerations drawn in the previous sections.

Hall Effect thrusters and **Ion thrusters** are rarely applicable and, when applicable, they never represent the preferred option. Their range of applicability is limited to larger satellites (3U and 12U) and to formation flying-related applications (altitude maintenance and station keeping).

Similar considerations apply to **Radio-Frequency thrusters** and to **resistojets** which, however, become in some cases a suitable solution for low-thrust Lunar transfer and attitude control in LEO, especially for the 12U format.

Electrospray, Pulsed Plasma Thrusters and **Vacuum Arc Thrusters** are characterized by a wide range of applicability to different applications and satellite formats. They represent the preferred solution for attitude control, low-thrust interplanetary transfer and, for smaller formats up to 3U, formation flying. In general it is apparent that, when a lower thrust level is acceptable or preferable, these electric propulsion options are clearly winning over any other micro-propulsion alternatives.

Due to their very poor performance in terms of specific impulse, **cold gas thrusters** do not have much applicability to the study cases considered in this Chapter. However, for larger satellite formats (3U and 12U), they represent a valid alternative to electric propulsion for low-thrust applications, in particular interplanetary transfer and attitude control.

Mono-propellant, bi-propellant and **solid propellant** options, due to their higher thrust levels, become attractive only for larger satellite formats (12U and, limited to the case of high-thrust Lunar transfer, 3U). In particular, it is interesting to note that mono-propellant thrusters represent the preferred option for formation flying applications (both low- and high-altitude) on the 12U format.

Looking at the applications, it can be observed that **attitude control in LEO** seems to not be feasible, at least with the requirements considered in this study, for the smaller satellite formats (3p and 1U). Same applies to **high-thrust interplanetary transfer**, while several options for **low-thrust interplanetary transfer** seem to be available for all satellite formats (except the 3p one).

To the contrary, **formation flying** applications (at both low and high altitude) seem to be widely feasible and several micro-propulsion options are available for them, for all the satellite formats considered in this study. This seems to confirm that the most promising application for this class of small satellites is represented by constellations, swarms and distributed systems of a large number of satellites, for which the availability of a propulsion system on-board of the satellite platform may make the difference and extend the range of possible missions and scientific objectives significantly.

Finally, looking at the satellite formats, it's evident that for the given applications a wide range of alternatives exist for the larger formats (3U and 12U), while very few options are available for the smaller ones (1U and 3p). This is not surprising, considering that the current state-of-art systems have been mostly designed for the 3U format or larger and do not easily match the characteristics of smaller formats. If popularity of these formats tends to increase in the next years, it will probably be necessary to develop new, dedicated micro-propulsion concepts to match their specific characteristics and requirements.

Table 4: Summary of the potential micro-propulsion applications for the 3p format

(● = applicable; O = partially applicable; coloured cells: preferred option).

Application	Hall Effect thruster	Ion thruster	RF thruster	Electrospray	Pulsed Plasma Thruster	Vacuum Arc thruster	Resistojet	Cold Gas	Mono-Propellant	Bi-Propellant	Solid Propellant
Attitude control in LEO (1-year orbital lifetime)											
Attitude control in LEO (5-years orbital lifetime)											
Orbit altitude maintenance in LEO (150 km altitude)											
Orbit altitude maintenance in LEO (300 km altitude)			●								
Station keeping in GEO			●			O					
Lunar transfer (low thrust)											
Lunar transfer (high thrust)											
Mars transfer (low thrust)											
Mars transfer (high thrust)											

Table 5: Summary of the potential micro-propulsion applications for the 1U format

(● = applicable; O = partially applicable; coloured cells: preferred option).

Application	Hall Effect thruster	Ion thruster	RF thruster	Electrospray	Pulsed Plasma Thruster	Vacuum Arc thruster	Resistojet	Cold Gas	Mono-Propellant	Bi-Propellant	Solid Propellant
Attitude control in LEO (1-year orbital lifetime)											
Attitude control in LEO (5-years orbital lifetime)											
Orbit altitude maintenance in LEO (150 km altitude)											
Orbit altitude maintenance in LEO (300 km altitude)			●								
Station keeping in GEO			●	●	●	O					
Lunar transfer (low thrust)			●	●	●						
Lunar transfer (high thrust)							O				
Mars transfer (low thrust)			●		●						
Mars transfer (high thrust)											

Table 6: Summary of the potential micro-propulsion applications for the 3U format

(● = applicable; O = partially applicable; coloured cells: preferred option).

Application	Hall Effect thruster	Ion thruster	RF thruster	Electrospray	Pulsed Plasma Thruster	Vacuum Arc thruster	Resistojet	Cold Gas	Mono-Propellant	Bi-Propellant	Solid Propellant
Attitude control in LEO (1-year orbital lifetime)				●	●	O					
Attitude control in LEO (5-years orbital lifetime)			O			O					
Orbit altitude maintenance in LEO (150 km altitude)											
Orbit altitude maintenance in LEO (300 km altitude)	●	O	●	●	●		O	O			O
Station keeping in GEO			●	●	●	●	O	O			●
Lunar transfer (low thrust)			●	●	●	●	●	●			
Lunar transfer (high thrust)									●	●	●
Mars transfer (low thrust)				●	●	●					
Mars transfer (high thrust)											

Table 7: Summary of the potential micro-propulsion applications for the 12U format

(● = applicable; O = partially applicable; coloured cells: preferred option).

Application	Hall Effect thruster	Ion thruster	RF thruster	Electrospray	Pulsed Plasma Thruster	Vacuum Arc thruster	Resistojet	Cold Gas	Mono-Propellant	Bi-Propellant	Solid Propellant
Attitude control in LEO (1-year orbital lifetime)			●	●	●	O	●	●	●	●	
Attitude control in LEO (5-years orbital lifetime)			●	●	●	O			●	●	●
Orbit altitude maintenance in LEO (150 km altitude)									●	●	●
Orbit altitude maintenance in LEO (300 km altitude)	●		●		●		O	O	●	●	●
Station keeping in GEO		●	●	●	●	●	●	O	●	●	●
Lunar transfer (low thrust)			●	●	●	●	●	●	●	●	
Lunar transfer (high thrust)											●
Mars transfer (low thrust)				●	●	●					
Mars transfer (high thrust)											

References

- [1] Heidt, H., et al., 2000, *CubeSat: a New Generation of Picosatellite for Education and Industry Low-Cost Space Experimentation*, Proceedings of the 14th AIAA/USU Conference on Small Satellites
- [2] Data from M. Swartwout, <https://sites.google.com/a/slu.edu/swartwout/home/cubesat-database> (last accessed: 22/05/2018)
- [3] Bayt R.L., 1999, *Analysis, Fabrication and Testing of a MEMS-based Micropulsion System*, PhD thesis, Massachusetts Institute of Technology
- [4] Levchenko, I., et al., 2018, *Space Micropulsion Systems for Cubesats and Small Satellites: from Proximate Targets to Furthermost Frontiers*, Applied Physics Reviews, 5(1)
- [5] Tummala, A.R., Dutta, A., 2017, *An Overview of Cube-Satellite Propulsion Technologies and Trends*, Aerospace, 4(4), 58
- [6] Krejci, D., Lozano, P., 2018, *Space Propulsion Technology for Small Spacecraft*, Proceedings of the IEEE, 106(3), 362-378
- [7] Silva, M.A.C., Guerrieri, D.C., Cervone, A., Gill, E., 2018, *A Review of MEMS Micropulsion Technologies for CubeSats and PocketQubes*, Acta Astronautica, 143, 234-243
- [8] Lemmer, C., 2017, *Propulsion for CubeSats*, Acta Astronautica, 134, 231-243
- [9] Parker, K.I., 2016, *State-of-the-Art for Small Satellite Propulsion Systems*, Proceedings of the 4th NSBE Aerospace Systems Conference
- [10] Leomanni, M., Garulli, A., Giannitrapani, A., Scortecci, F., 2017, *Propulsion Options for Very Low Earth Orbit Microsatellites*, Acta Astronautica, 133, 444-454
- [11] Larson, W. J., Wertz, J.R., 1992, *Space Mission Analysis and Design*, 3rd edition, Microcosm, Inc., Torrance, CA
- [12] Silva, M.A.C., Guerrieri, D.C., van Zeijl, H., Cervone, A., Gill, E., 2017, *Vaporizing Liquid Microthrusters with Integrated Heaters and Temperature Measurement*, Sensors & Actuators: A. Physical, 265, 261-274
- [13] Guerrieri, D.C., Silva, M.A.C., Cervone, A., Gill, E., 2017, *Selection and Characterization of Green Propellants for Micro-Resistojets*, ASME Journal of Heat Transfer, 139(10)
- [14] Guerrieri, D.C., Silva, M.A.C., van Zeijl, H., Cervone, A., Gill, E., 2017, *Fabrication and Characterization of Low-Pressure Micro-Resistojets with Integrated Heater and Temperature Measurement*, Journal of Micromechanics and Microengineering, 27.12
- [15] Sutton, G.P., 1978, *Rocket Propulsion Elements*, 7th edition, John Wiley & Sons Inc.
- [16] Hill, P.G., Peterson C.R., 1992, *Mechanics and Thermodynamics of Propulsion*, Addison-Wesley Publishing Co.
- [17] Levchenko, I., et al., 2020, *Perspectives, Frontiers and New Horizons for Plasma-Based Space Electric Propulsion*, Phys. Plasmas, 27 020601
- [18] Ganani, C.S., Cervone, A., 2019, *Performance Improvement of MEMS Micro-Thrusters Through Novel Double Depth Aerospike Design*, IAF 70th International Astronautical Congress, Washington, DC, USA